Influence of the nuclear medium on the structure of bound nucleons

I. A. Savin and G. I. Smirnov
Joint Institute for Nuclear Research, Dubna

Fiz. Elem. Chastits At. Yadra **22**, 1005–1066 (September–October 1991)

The paper reviews experimental studies of the distortion of nucleon structure by the surrounding nuclear medium, or the so-called nuclear effects in structure functions. These distortions were first observed by the European Muon Collaboration in measurement of the nucleon structure functions in the nuclei of deuterium and iron and have become known as the EMC effect. The review also includes the results of experiments on deep inelastic scattering of muons, electrons, neutrinos, and antineutrinos by nucleons in nuclei and also studies of other reactions: the production of massive lepton pairs and J/ψ particles and the interaction of hadrons with nuclei. The experimental data are compared with the corresponding calculations of several theoretical models of nuclear structure proposed to explain the EMC effect. The high accuracy of the experiments permits the conclusion that some models "guess" qualitative features of the effect, but none of them gives a satisfactory description of all the experimental data. Kinematic regions in which further critical tests of these models are possible are indicated.

INTRODUCTION

It is well known that experiments in which leptons (electrons, muons, neutrinos) are scattered by nucleons and nuclei make it possible to probe their structure. The advantage of leptons over other probes is that the leptons themselves, according to existing experimental data,[1] do not possess structure (they are point particles) and therefore do not introduce uncertainties into the measurements. At the same time, the scattering cross sections have a simple theoretical interpretation—apart from the radiative corrections, they can be compared with phenomenological functions that characterize the nucleon structure. Thus, in elastic and inelastic lepton–nucleon scattering, the scattering cross sections are proportional to the electric, $G_E(Q^2)$, and magnetic, $G_M(Q^2)$, nucleon form factors[2,3] (Q^2 is the square of the 4-momentum transferred to a nucleon by a virtual photon). In the analogous data on deep inelastic scattering, when the 4-momentum transfer satisfies $Q^2 \gg M^2$, where M is the nucleon mass, the cross sections can be expressed in terms of the nucleon inelastic structure functions $F_i(x,Q^2)$, $i = 1, 2, 3$,[4] and these are, on the basis of modern ideas about the structure of matter, related to the distributions with respect to the corresponding variables of the partons, the point objects that make up nucleons and are called the nucleon constituents. The variable x determines the fraction of the nucleon momentum carried away by a parton. Experiments on the deep inelastic scattering of leptons by nucleons showed that the partons possess properties identical to those of the quarks postulated by Gell-Mann[5] and Zweig[6] to explain the results of hadron spectroscopy experiments.

One of the first discoveries in investigations of deep inelastic scattering of electrons by protons was the scaling of the structure functions predicted by Bjorken.[7] His conjecture takes this form: When the energy transfer $\nu = E - E'$, where E and E' are, respectively, the energy of the incident and scattered lepton in the laboratory frame, and the 4-momentum Q^2 tend to infinity, the dependence of the structure functions on Q^2 should disappear:

$$F_i(x,Q^2)\,|_{\nu,Q^2\to\infty} \to F_i(x). \tag{1}$$

Such behavior was discovered in a series of famous experiments[8] with the linear electron accelerator (SLAC) at the Stanford National Laboratory already at $Q^2 = 2$–$10\,\mathrm{GeV}^2$.

Scaling has a simple explanation in the framework of the quark–parton model,[9] in which the nucleon structure functions can be expressed in terms of the quark, $q_f(x)$, and antiquark, $\bar{q}_f(x)$, distributions:

$$2xF_1(x) = F_2(x) = \sum_f e_f^2 x[q_f(x) + \bar{q}_f(x)], \tag{2}$$

where e_f is the charge of the quark (and antiquark) with flavor f.

For an accurate test of the quark–parton model, it would be necessary to study deep inelastic scattering of leptons in a wide range of Q^2, including values $Q^2 > 10\ \mathrm{GeV}^2$. However, the cross sections of lepton–nucleon scattering measured at such transfers are less than $10^{-33}\ \mathrm{cm}^2$. Therefore, to ensure a high statistical accuracy during a reasonable time of measurements, nuclear targets, rather than nucleons, were used in most of the experiments. It was assumed that the structure functions measured in this case for a nucleon bound in a nucleus A, $F_i^A(x,Q^2)$, are identical to the structure functions of a free nucleon of an isoscalar target: $F_i^N = (1/A)F_i^A$, where F_i^N are defined as the half-sums of the structure functions of the free neutron and free proton:

$$F_i^N(x,Q^2) = (1/2)[F_i^p(x,Q^2) + F_i^n(x,Q^2)]. \tag{3}$$

The results of numerous experiments on deep inelastic scattering of leptons by nuclei made up to 1983 in the interval $0.1 < x < 0.7$ were analyzed in the framework of this approach. It was found that the scaling hypothesis is satisfied only in a restricted range of x ($x \sim 0.2$–0.3). The

observed violations of scaling are characterized by a growth of the structure functions with increasing Q^2 in the region $x \lesssim 0.2$ and a decrease of them at $x \gtrsim 0.3$. The same functional dependences of the scaling violations were obtained, within the errors of the measurements, in experiments using different nuclei.

The assumption that the structure functions of the free nucleon and of the nucleon bound in a nucleus are identical was first directly tested by the European Muon Collaboration[10] in the region $x < 0.7$, in which the effect of the motion of the nucleons in a nucleus are still weak. Using a muon beam from the SPS accelerator at CERN, the Euproean Muon Collaboration made measurements of the structure function of a nucleon in the nuclei of iron (F_2^{Fe}) and deuterium (F_2^{D}) and their ratio:

$$r^{\mathrm{Fe}}(x) = F_2^{\mathrm{Fe}}(x)/F_2^{\mathrm{D}}(x). \tag{4}$$

In the deuterium nucleus, the nucleons are weakly bound, and to good accuracy $(1/2)F_2^{\mathrm{D}} = F_2^{\mathrm{N}}$, where F_2^{N} is determined by the expression (3).

Instead of the approximate equality $r^{\mathrm{Fe}}(x) \approx 1.0$ expected in the region $x \in (0.1, 0.7)$ the ratio (4) decreases linearly with increasing x. This result became known as the EMC effect. The results of the EMC experiment not only indicated that the nuclear medium can influence the nucleon properties but they also became, admittedly with large errors, the first quantitative measurement of the degree of distortion of the internal structure of a nucleon in a nucleus. The exceptional importance of these results stimulated rapid development of more accurate experimental investigations of the effect, and also the development of a theoretical formalism for its explanation. All the experimental facilities in Europe and the United States possessing capabilities for carrying out experiments on deep inelastic scattering of leptons by nuclei were used to test and study in detail this fundamental phenomenon. Experiments were made using electron, muon, and neutrino beams.

The most accurate results, which became the basis for comparison with theoretical calculations, were obtained at CERN by the BCDMS collaboration, and also at SLAC by a group that included physicists from SLAC, MIT, FNAL, and a number of universities in the United States. These groups confirmed and measured more precisely the effect with an accuracy that was a record for experiments of such complexity involving measurements of the ratios of the structure functions of nucleons bound in nuclei and free nucleons, namely, of order 1%.

Earlier investigations of hadron–nucleus interactions had also observed differences in the behavior of the cross sections measured on heavy and light nuclei.[11] Despite the difficulty in interpreting hadron–nucleus reactions, the results of many experiments convincingly demonstrated qualitative agreement of the nuclear effects found in deep inelastic scattering of leptons and in hadron–nucleus processes.

Numerous attempts were made to explain the nuclear effects observed in the experiments. On the basis of the already developed models of nuclear structure, the theoreticians were quite soon able to describe qualitatively individual aspects of the behavior of the structure-function ratios. However, taking into account the achieved experimental accuracy, one can say that none of the proposed models can as yet pretend to a quantitative description of the complete effect. Thus, the question of the nature of the considered effect remains open. There is no doubt that subsequent investigations of the structure functions by means of deep inelastic scattering of leptons will stimulate the development of a quark theory of nuclear matter and, possibly, explain the nature and basic properties of nuclear forces.[12]

The present review is based on studies aimed at finding and investigating differences in the structure functions of free and bound nucleons, and also in the cross sections for scattering of leptons and hadrons by free and bound nucleons. Sections 1 and 2 contain a detailed exposition of the history and ways in which nucleon structure has been studied. Section 3 describes the EMC experiment, which initiated the intensive study of the influence of the nuclear medium on nucleon structure, and Sec. 4 describes the experiments on the deep inelastic scattering of leptons by nuclei that confirmed and established more accurately specific features of the EMC effect. Other nuclear effects observed in hadron–hadron and lepton–hadron collisions are considered in Sec. 5. Section 6, which does not pretend to completeness, contains an analysis of theoretical studies initiated by the discovery of the EMC effect.

1. LEPTON SCATTERING AS A TOOL FOR STUDYING NUCLEON STRUCTURE

The investigations of nucleon structure made during the last three decades with lepton beams can be divided into three stages, each of which was associated with a new discovery.

The first stage includes experiments on inelastic scattering of 188-MeV electrons by protons,[13] and also inelastic *ep* scattering experiments at 1200 MeV (Ref. 14). These experiments showed that the electric and magnetic charges of the nucleon are not concentrated at a point but are characterized by a spatial distribution, namely, by the electric, $G_E(Q^2)$, and magnetic, $G_M(Q^2)$, form factors.

The typical distances at which the structure of the particles was probed in these experiments are characterized, for example, by the proton rms radius[13]

$$\langle r_p \rangle^{1/2} = (0.74 \pm 0.24) \cdot 10^{-13}\ \mathrm{cm}.$$

In other words, it was found that the nucleon elementary particle has a radius $r_N \sim 10^{-13}$ cm.

Simultaneously with the experiments to measure the nucleon form factors $G(Q^2)$, there were experiments to investigate the structure of the proton by means of elastic scattering of 100-MeV photons. In accordance with the theoretical estimates made in Ref. 15, the spatial structure of the proton should be manifested in subtle effects—electric and magnetic polarizability of it. The experiments made with the electron synchrotron of the P. N. Lebedev Physics Institute revealed the predicted effects and provided important quantitative information about the electromagnetic properties of the proton.[16,17]

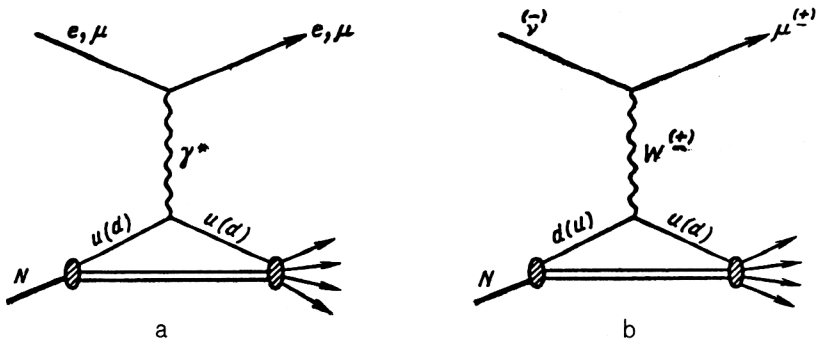

FIG. 1. Diagrams making the main contribution to the cross sections for deep inelastic scattering of the leptons e and μ (a) and ν (b) by the nucleon N.

The discovery of internal structure of an elementary particle and the introduction of the concept of a form factor that depends on the momentum transfers to the nucleon had truly revolutionary significance for theoretical physics, which had previously considered interaction of fields only with point particles. (Ref. 18).[1)]

The second stage of investigations of nucleon structure was associated with the linear electron accelerator SLAC at Stanford in the United States, with which in 1969 electrons were accelerated to 18 GeV. The attainment of this energy made possible deep inelastic reactions with large energy and momentum transfer from an electron to a target nucleon, resulting in copious production of secondary hadrons. Detection of secondary hadrons is not necessary to study the properties of the nucleon. Such reactions without detection of the secondary hadrons are called inclusive and are expressed in the form

$$e^- + N \to e^- + X, \tag{5}$$

where X are the undetected reaction products.

The commissioning of accelerators with muon and neutrino beams at Fermilab and CERN opened up new possibilities for investigating deep inelastic scattering of leptons by nucleons and nuclei in the following reactions:

$$\mu^\pm + N(A) \to \mu^\pm + X; \tag{6}$$

$$\nu + N(A) \to \mu^- + X; \tag{7}$$

$$\bar{\nu} + N(A) \to \mu^+ + X. \tag{8}$$

These reactions can be described by means of the diagrams in Fig. 1. It can be seen from Fig. 1a that for the processes (5) and (6) it is the virtual proton γ^* that plays the part of a probe, while for the processes (7) and (8) it is the intermediate charged boson W (Fig. 1b).[2)]

Just as the resolution of an optical instrument increases with decreasing wavelength of the light that it uses, the method of deep inelastic scattering of leptons by nucleons has a resolution that depends on the mass of the virtual photon (or on the square Q^2 of its 4-momentum):

$$\Delta l \sim 1/\sqrt{Q^2},$$

where

$$Q^2 = -q^2 = -(p-p')^2 = 4EE' \sin^2(\theta/2),$$
$$Q^2_{\max} = 2ME. \tag{9}$$

Here, p, p' and E, E' are the c.m.s. momenta and energies of the incident and scattered lepton, respectively, M is the nucleon mass, and θ is the c.m.s. emission angle of the scattered lepton. Thus, as the maximal squared 4-momentum transfer $Q^2_{\max}$ attainable in an experiment is increased, the structure of the nucleon is probed to ever shorter distances $r \approx \Delta l$.

In the SLAC experiments it was possible to investigate nucleon structure at distances of order 3×10^{-15} cm, and this made it possible to discover strong differences in the Q^2 dependence of the elastic and inelastic electron–nucleon scattering cross sections. Instead of the $1/Q^8$ decrease of the cross section with increasing 4-momentum transfer characteristic of a spatial nucleon charge distribution in a sphere with radius r_N, the deep inelastic scattering cross sections were found to depend on the 4-momentum transfer as $1/Q^4$ (Ref. 8). The results of these experiments demonstrated the existence within the nucleon of pointlike charged objects, which were called partons.

The phenomenon of Bjorken scaling found in the SLAC experiments in the comparatively small interval of squared momentum transfers up to $Q^2 \sim 8$ GeV^2 gave a powerful stimulus to the development and testing of the quark–parton model. The deviations from scaling in the wider range up to $Q^2 \sim 20$ GeV^2, also observed at SLAC and then confirmed at Fermilab and CERN in the muon and neutrino beams, indicated a lepton–nucleon interaction mechanism different from the one proposed in the framework of the quark–parton model. Thus, the second stage in the study of nucleon structure ended with the formulation of the problem of high-precision investigations into the properties of the nucleon constituents and the manner in which scaling is violated.

Quantum chromodynamics predicts a specific form of scaling violation.[22] According to it, the structure functions depend logarithmically on the squared 4-momentum transfer: $F_i(x,Q^2) \sim \ln(Q^2/\Lambda^2)$, where Λ is a scale parameter of the theory determined experimentally. The testing of this prediction required experiments to be made in the widest possible range of Q^2. To realize the new experimental program, it was necessary to create high-quality muon and neutrino beams at Fermilab and CERN, and also high-luminosity spectrometers for detection of deep inelastic scattering of muons from the reactions (6)–(8).

In the third stage of investigations of nucleon struc-

ture, which began at the end of the seventies, we must include the high-precision experiments made with the CDHS, CHARM, EMC, and BCDMS facilities at CERN, the BFP and CCFR facilities are Fermilab, and also the new generation of experiments at SLAC. During the course of these experiments, carried out during the last decade, several fundamental discoveries were made. It was established that: 1) in the nucleon there are three valence quarks of type u and d, and also a sea of the virtual quarks and antiquarks u, d, s, c, etc; 2) quarks are point particles possessing fractional electric charge and spin 1/2; 3) the quarks in the gluon are held ("glued") together by means of neutral gluons.[23] The x distributions of the individual quark species were determined. The violation of CP invariance in deep inelastic scattering of longitudinally polarized electrons and muons predicted by the standard model was found. It was shown that in the range $1 < Q^2 < 300$ GeV^2, currently accessible in fixed-target experiments, scaling is violated in accordance with the QCD predictions. According to the most accurate measurements of the BCDMS collaboration,[24] the parameter $\Lambda_{\overline{\rm MS}}$ of the theory is 220 ± 15 MeV. Finally, it was established that the properties of free nucleons and nucleons bound in a nucleus are different.

This is by no means a complete list of the results of the third stage, which, in its turn, posed new problems, including problems of detailed study of the quark properties of nuclei.

2. DEEP INELASTIC LEPTON SCATTERING CROSS SECTIONS

In this section, we shall give only basic equations. If necessary, the reader should refer to the special literature (for example, Ref. 2) or reviews (for example, Ref. 23).

It is customary to represent the cross section for deep inelastic scattering of electrons and muons by the nucleon in the single-photon approximation. This cross section can be calculated with an uncertainty of a few percent[3)] for a large part of the range of variation of the kinematic variables x and y:

$$\frac{d^2\sigma}{dxdy}=\frac{4\pi\alpha^2}{Q^4}ME\left[xyF_1(x,Q^2)+\left(1-y-\frac{Mxy}{2E}\right)F_2(x,Q^2)\right] \tag{10}$$

Here, $x = Q^2/2M\nu$, $\nu = E - E'$, $y = \nu/E$, and F_1 and F_2 are the nucleon structure functions, which depend on two variables. In the framework of the quark–parton model, the expressions for the structure functions in terms of the parton distributions depend on the target nucleus. For example, if the standard fractional charges are ascribed to the u, d, s, and c quarks, then for scattering of electrons or muons by hydrogen or by a nucleon of an isoscalar target they have the form

$$F_2^{ep}(x)=\tfrac{5}{18}x\Sigma(x)+\tfrac{1}{6}x\Delta^{ep}(x); \tag{11}$$

$$F_2^{eN}(x)=\tfrac{5}{18}x\Sigma(x)+\tfrac{1}{6}x\Delta^{en}(x), \tag{12}$$

where $\Sigma(x) = q(x) + \bar{q}(x)$ is the so-called SU(4)-singlet quark–antiquark distribution, and $\Delta(x)$ is the nonsinglet distribution:

$$\Delta^{ep}=\Delta^{eN}+(u-d)+(\bar{u}-\bar{d}),$$

$$\Delta^{eN}=(\bar{c}-\bar{s})+(c-s).$$

On transition to the process (7) of deep inelastic neutrino–nucleon scattering, it is necessary to replace in the calculations[4] the electromagnetic current by the weak current, and then in the one-boson approximation the cross section takes the form

$$\left(\frac{d^2\sigma}{dxdy}\right)^{\nu(\bar{\nu})}=\frac{G^2ME}{\pi}\left[xy^2F_1(x,Q^2)+\left(1-y-\frac{Mxy}{2E}\right)F_2(x,Q^2)\pm y\left(1-\frac{y}{2}\right)xF_3(x,Q^2)\right], \tag{13}$$

where the structure function F_3 appears because of the details of weak interactions, and the sign in front of the term containing F_3 is changed from $+$ for ν to $-$ for $\bar{\nu}$.

In the framework of the quark–parton model and the standard model of weak interactions, the cross sections of the processes (7) and (8) due to charged currents (CC) can be expressed in terms of the parton distributions. For an isoscalar target, they have the form[4]

$$\left(\frac{d^2\sigma}{dxdy}\right)^{\nu N}_{CC}=\frac{G^2ME}{\pi}x\{[q(x)+s(x)-c(x)]+(1-y)^2[\bar{q}(x)+\bar{c}(x)-\bar{s}(x)]\}; \tag{13a}$$

$$\left(\frac{d^2\sigma}{dxdy}\right)^{\bar{\nu}N}_{CC}=\frac{G^2ME}{\pi}x\{[\bar{q}(x)+\bar{s}(x)-\bar{c}(x)]+(1-y)^2[q(x)+c(x)-s(x)]\}. \tag{13b}$$

Comparing these expressions with (13), we see that

$$2xF_1^{\nu(\bar{\nu})N}=F_2^{\nu(\bar{\nu})N}=x\Sigma(x),\quad xF_3^{\nu(\bar{\nu})N}=xV(x)\pm x\Delta^{eN},$$

i.e., $F_2^{\nu(\bar{\nu})N}$ behaves as a purely singlet function, and $xF_3^{\nu(\bar{\nu})N}$ as a purely-nonsinglet function effectively determined by the distribution $V(x)$ of the valence quarks alone because Δ^{eN} is small.

The kinematics of the processes (5)–(8) for the case of deep inelastic scattering on nuclei are different in that the range of the variable x is no longer the (0, 1) for the nucleon but (0, A) for the nucleus, i.e., the expressions (10) and (13) can be used to calculate the cross sections for interaction on one nucleon of the nucleus after the substitutions $x \to x_A$ and $F_i(x,Q^2) \to F_i^A(x_A,Q^2)$, $i = 1, 2, 3$.

In the general case, the virtual photon is characterized by longitudinal and transverse polarizations,[26] and this

makes it possible to separate in the expression (10) for the cross section two parts corresponding to the cross sections for absorption of transversely (σ_T) and longitudinally (σ_L) polarized photons. However, one often makes a restriction to study of their ratio $R(x,Q^2)$:

$$R(x,Q^2)\equiv\frac{\sigma_L}{\sigma_T}=\frac{F_2(x,Q^2)(1+4M^2x^2/Q^2)-2xF_1(x,Q^2)}{2xF_1(x,Q^2)}, \tag{14}$$

which makes it possible to represent the cross section for deep inelastic scattering of electrons or muons as a function of $F_2(x,Q^2)$ and $R(x,Q^2)$.

On the transition from the virtual photon in the processes (5) and (6) to the intermediate W boson in the processes (7) and (8), it is not possible to make a complete analogy for the parameter $R(x,Q^2)$, but the use of the quark–parton model makes it possible for the neutrino deep inelastic scattering cross section too to separate a part of it proportional to the longitudinal cross section σ_L (see Sec. 4).

3. DISCOVERY OF THE EMC EFFECT

Before the publication of the EMC collaboration[10] of the discovery of differences between the x dependences of the structure functions of deuterium and iron, solid (nuclear) targets were used in investigations of lepton deep inelastic scattering in order to increase the luminosity of the experimental facility (and not to study nuclear structure). Indeed, in a deep inelastic reaction, the momentum transfer from the lepton to the nucleon is $k=\sqrt{Q^2}$, and this exceeds by 3–4 orders of magnitude the binding energy of the nucleon in the nucleus and is about two orders of magnitude higher than the mean nucleon Fermi momentum. Under these conditions, it is hard to expect nuclear structure effects to have a significant influence on the lepton scattering cross section. There were also experimental indications that the cross section of the reaction (5) on nuclei was directly proportional to the sum of the cross sections on the individual nucleons forming the nucleus. Such a result was obtained at SLAC,[27] in which scattering of electrons with energy from 4.5 to 19.5 GeV was studied on the nuclei of hydrogen, deuterium, beryllium, aluminum, copper, and gold.

Thus, there were grounds were believing that in the greater part of the kinematic range of the variables x and Q^2 that is accessible in lepton deep inelastic scattering, or at least in the range of x from 0.05 to 0.7, the following conditions would hold:

1) the virtual photons (bosons) would be scattered incoherently by nuclear nucleons at rest:

$$AF_i^A(x,Q^2)=ZF_i^p(x,Q^2)+(A-Z)F_i^n(x,Q^2); \tag{15a}$$

2) nuclei could be assumed to be approximately isoscalar: $A\approx 2Z$, i.e.,

$$F_i^A(x,Q^2)=\frac{A}{2}F_i^D(x,Q^2); \tag{15b}$$

3) the parameter $R=\sigma_L/\sigma_T$ could be expected to be approximately constant for all nuclei, being a function of only x and Q^2.

For $x<0.05$, it was expected that screening effects would reduce the cross section for deep inelastic scattering by a nucleus compared with the free nucleon:[28]

$$\sigma^A<A\sigma^N. \tag{16}$$

In contrast, in the region $x>0.7$ it was expected[26] that

$$\sigma^A>A\sigma^N. \tag{17}$$

The relation (17) follows because when the variable x tends to the kinematic limit $x=1.0$ the nuclear structure functions $F_i^A(x)$ begin to exceed $F_i^N(x)$, since

$$F_2^A(x,Q^2)=\int_{z>x}dzF_2^N(x/z,Q^2)f_N(z),$$
$$xF_i^A(x,Q^2)=\int_{z>x}dz(x/z)F_i^N(x/z,Q^2)f_N(z),\quad i=1,3, \tag{18}$$

where $f_N(z)$, the momentum distribution of the nucleons in the nucleus, is nonzero for $x=1$.

The EMC experiment

For many years, the low statistical and, in particular, systematic accuracy with which the nucleon structure functions were measured in lepton deep inelastic scattering experiments meant that it was not possible to establish reliably the extent to which the relations (15)–(18) were satisfied. First results on their quantitative verification in the region $x\in(0.05, 0.65)$ were obtained at CERN by the EMC collaboration.[10] In this experiment, the reaction (6) was studied on an iron target at energies 100, 120, 250, and 280 GeV, and also on a deuterium target at energy 280 GeV. From the resulting data, using the relations (10) and (14), the structure functions F_2^{Fe} and F_2^D were calculated under the assumption that $R=\sigma_L/\sigma_T=0$. This was justified by measurements of the same group on the iron target: $R=0.03\pm0.12$. The structure functions F_2^{Fe} and F_2^D were compared in the range $0.03<x\leqslant 0.65$. Instead of the expected equality of the structure functions $F_2^{Fe}(x,Q^2)$ and $F_2^D(x,Q^2)$ in the complete studied range of the variable x, they were found to be equal only for $x\approx 0.3$. At smaller values of x, it was found in the complete range of Q^2 that $F_2^{Fe}>F_2^D$, while for $x>0.3$ it was found that $F_2^{Fe}<F_2^D$. Since no significant Q^2 dependence of the ratio (4) was found within the statistical and systematic errors, the data were integrated over the region $9<Q^2<170$ GeV^2 in order to study the x dependence of the ratio with greater accuracy. In addition, corrections were introduced to allow for the nonisoscalar nature of the iron nucleus, this being done under the assumption that the proton and neutron structure functions were related by $F_2^n=(1-0.75x)F_2^p$. The inaccuracy of this assumption had little influence on the correction, which is 2.3% for $x=0.65$ and does not exceed 1% for $x<0.3$. The result obtained[10] for the ratio r^A—it soon became known as the "EMC effect"—is shown in Fig. 2 together with the estimates of the systematic errors taken from Ref. 29. In order to fit the relation (4), the authors

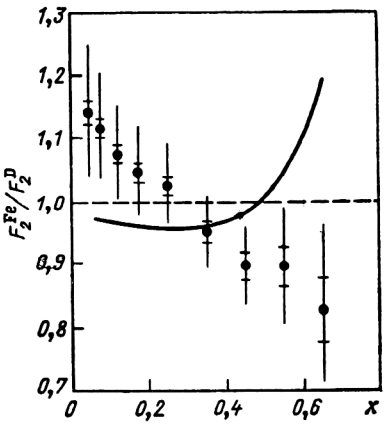

FIG. 2. Ratio of nucleon structure functions measured in the EMC experiment[10,29] on iron and deuterium nuclei. The behavior of this ratio expected on the basis of consideration of nucleon Fermi motion in the nucleus is shown by the continuous curve.

made the hypothesis of a decrease of r^A with increasing x in accordance with the linear law $r^A = a + bx$ and obtained $b = -0.52 \pm 0.04_{\text{stat}} \pm 0.21_{\text{syst}}$ (the EMC collaboration did not publish an estimate of the parameter a).

Despite the appreciable experimental errors, the authors concluded that the x dependence of the ratio r^A contradicted calculations in which the differences in the iron and deuterium structure functions were ascribed to the influence of the Fermi motion of the nucleons in the nucleus.[30] For example, instead of the expected growth of r^A to ~ 1.2 at $x = 0.65$, a decrease of r^A to about 0.89 was observed. Especially intriguing was the indication of a growth of r^A to 1.15 at $x = 0.05$. Since in the framework of the quark–parton model the structure function $F_2(x)$ is related to the momentum distributions (2) of the quarks and antiquarks in the nucleon, the existence of the EMC effect could mean that these distributions are changed by the nuclear medium.

Before we turn to further discussions of the phenomenon, it is expedient to dwell on the specifics of the measurement of the nuclear and nucleon structure functions and their ratio. This will enable us to understand the significance of the numerous experiments made after the EMC experiment.

As we mentioned above, for many years the appreciable experimental errors, above all the statistical errors, made it impossible to discover any significant differences between the structure functions of free and bound nucleons. The desire of the experimentalists to raise the statistical accuracy of their experiments led to a lengthening of the time of data collection and to the appearance of additional systematic errors, which often exceeded the statistical errors.

Except for the MIT–SLAC[31] and Rochester–MIT–SLAC[32,33] experiments, the measurements of the structure functions on different nuclei were made in different experiments and at different times. Under such conditions, it is difficult, and often impossible, to control the systematic errors which arise from the conditions under which the experiments are made. The differences and instabilities in the phase spaces of the beams of incident particles, the differences in the efficiencies of the detecting apparatus, in the geometry of the targets, and in their capacity to absorb secondary particles, and also the differences in the acceptances of the experimental facilities led to systematic errors not only in the absolute cross sections but also in the distributions of the detected events with respect to the kinematic variables.

The EMC collaboration encountered just such difficulties in the comparisons of the structure functions on the iron and deuterium nuclei. The experimental data were obtained at different muon energies at different times, i.e., effectively in different experiments. This cast doubt on the reliability of the result, since it certainly had to contain large systematic errors. Although they had discovered differences between the structure functions F_2^{Fe} and F_2^D already in 1981,[34] the EMC collaboration made considerable efforts to verify the result carefully,[35] which was published only in 1983.[10]

The experiment of the Rochester–MIT–SLAC group

The highest accuracy in measurements of structure functions that preceded the EMC measurements was achieved by the Rochester–MIT–SLAC collaboration.[32,33] In this experiment, the method of frequent changing of the targets was used in order to reduce the systematic errors. Three targets of identical shape were placed in an electron beam by remote control. Two targets were filled with liquid hydrogen and deuterium, and the third—a hollow iron cylinder—was left empty to make background measurements. The results of this experiment, which contained values of the neutron and proton structure functions, were published in 1974. Immediately after the first communication[35] of the EMC results, the same group reanalyzed archival data of the measurements on the hollow iron cylinder as independent measurements of the cross sections and compared the σ^{Fe} obtained in this manner with σ^D. In the region $x > 0.3$ and $Q^2 = 4$–21 GeV^2, they also found a decrease of $r^A(x)$ with increasing x, as in the EMC effect.[36] This result was, despite its unusual history, regarded as a first confirmation of the EMC results. Even more convincing evidence for the effect was obtained as a result of reanalysis of data of a different experiment that had been made earlier at SLAC in order to compare the structure functions of the neutron and proton.[37] Targets made of aluminum had been used in that experiment. This provided a possibility to demonstrate that the structure functions of the nucleon in the aluminum nucleus are distorted in approximately the same way as in the iron nucleus.[38] The results of analysis of the SLAC archival data are shown in Fig. 3.

If a restriction is made to the range of variation of the variable x from 0.2 to 0.6, the ratio $r^A(x)$ can be well described by a straight line with the parameters given in Table I.

Because the range of measurements with respect to x

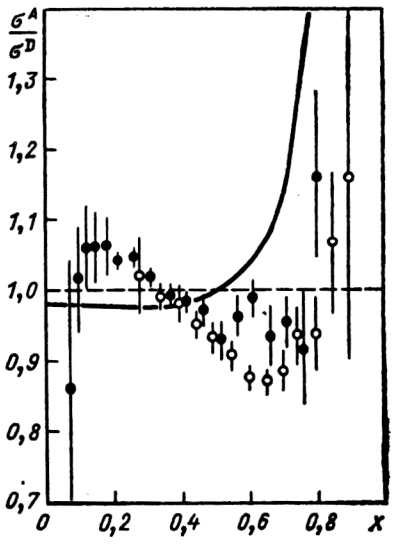

FIG. 3. Cross section ratios σ^{Fe}/σ^{D} (open circles) and σ^{Al}/σ^{D} (black circles) measured by the Rochester–MIT–SLAC collaboration on deuterium and on the walls of empty, aluminum,[38] and iron[36] targets. The continuous curve shows the result of a calculation of σ^{Fe}/σ^{D} made with allowance for only Fermi motion of a nucleon in the nucleus.

has been extended from that in the EMC work, Fig. 3 reveals new manifestations of nuclear effects in the interaction cross section, namely, the ratio $r^{A}(x)$ reaches a minimum at $x \approx 0.65$–0.7 and then, as follows from (18), begins to increase rapidly.

4. INVESTIGATION OF NUCLEAR EFFECTS IN THE STRUCTURE FUNCTIONS

The next logical step after the discovery of the new effect was detailed study of it in order to establish its form and the reasons for its occurrence. In this section, we shall show how the experimental investigations of the EMC effect in electron, muon, and neutrino beams developed, and also how the experiments set up during 1983–1988 determined the dependence $r^{A}(x)$ more accurately.

TABLE I. The parameters a and b and their errors Δa and Δb obtained by fitting results of measurements on the Al and Fe nuclei by the dependence $r_A = a + bx$.

Parameter	Target		
	Al/D (Ref. 38)	Fe/D (Ref. 36)	Fe/D (Ref. 29)
a	1.11	1.15	1.17
Δa	0.02	0.04	—
b	−0.30	−0.45	−0.52
Δb	0.06	0.08	0.04

As we noted in Sec. 2, the lepton deep inelastic scattering cross sections and structure functions are described by two independent kinematic variables. These can be the variable pairs (Q^2,x), (Q^2,ν), or (x,y). Because the EMC effect is a nuclear effect, it is also natural to consider the dependence of the scattering cross sections and structure functions of the nucleons on the mass number A of the target nucleus. For this reason, the detailed investigations of the EMC effect consisted of study of the ratio of the structure functions F_2^A and F_2^D or of the cross sections σ^{A} and σ^{D} as functions of the variables x, y, or Q^2 and of A.

Dependence of the nuclear effects on the Bjorken variable x

The experiment of the SLAC–MIT group[39] was the first post-EMC experiment made specially to study $r^{A}(x,Q^2)$ in terms of the cross-section ratio,

$$r^{A}(x,Q^2) = \sigma^{A}(x,Q^2)/\sigma^{D}(x,Q^2), \tag{19}$$

with precautionary measures taken to lower the possible systematic errors. The estimates showed that the system-

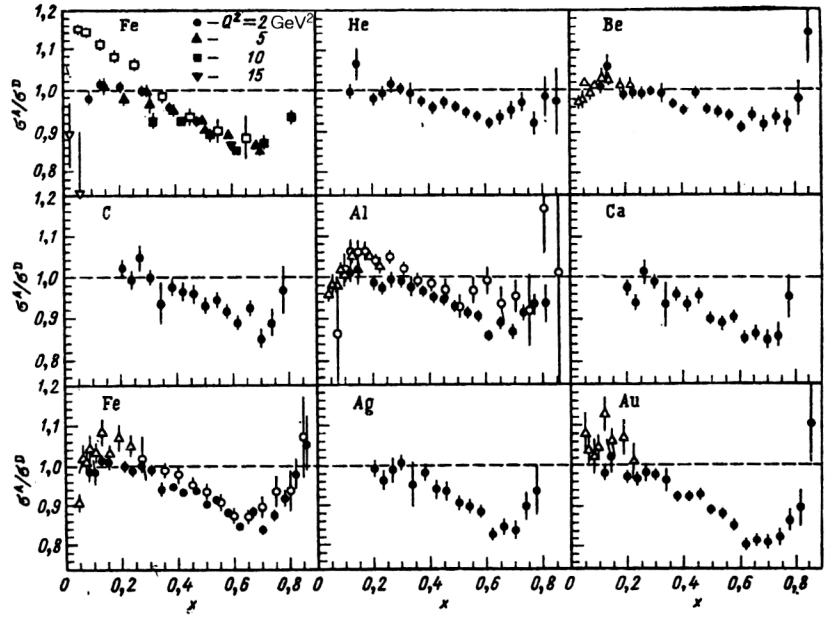

FIG. 4. Ratios of cross sections for deep inelastic scattering of electrons by nuclei obtained in the SLAC experiment[39] (black circles). Also shown are results of the EMC experiment on iron[10] (open squares) and early SLAC experiments on beryllium, aluminum, iron, copper, and gold: open circles (Refs. 36 and 38), open triangles (Ref. 50), open inverted triangles (Ref. 84). The results of the experiments of Refs. 50 and 84 on a copper target are shown together with the results of Ref. 39 obtained on an iron target.

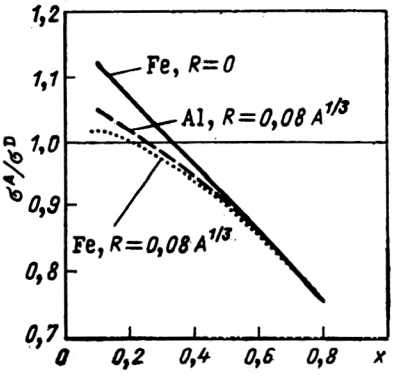

FIG. 5. Cross-section ratios σ^A/σ^D calculated for the same ratio $F_2^A/F_2^D = 1.17 - 0.52x$ of the structure functions but for different $R = \sigma_L/\sigma_T$.

atic errors in r^A were approximately the same from point to point and, like the systematic errors in the data normalization, did not exceed 2%. From Fig. 4, which shows the results of the measurements, it can be seen in the first place that for Q^2 equal to 2, 5, 10, and 15 GeV^2 the ratios r^{Fe} are the same within the errors. This justified integration of the data over Q^2 and consideration of only the x dependence of r^A for all nuclei. It can also be seen that in the range $0.3 < x < 0.7$ there is good agreement for r^{Fe} with the EMC results. But in the region of smaller x, the SLAC–MIT data for r^{Fe}, obtained with lower errors than for the EMC data, contradicted those data—instead of a growth, the ratio r^{Fe} "flattened" at the level $r^{Fe} \approx 1.0$. A similar tendency can also be seen for other nuclei. Only new high-precision experiments could resolve this contradiction.

As a result of these measurements, the data also reliably established for all nuclei the existence of the minimimum in $r^A(x)$ at $x \sim 0.65$ that had first been noted in SLAC archival data.[36,38] We shall discuss the A dependence of the features noted here below.

In discussions in the literature of the discrepancies between the EMC and SLAC–MIT data in the range $x < 0.3$, it was pointed out that the ratios (4) and (19) need not be equal. As follows from (10) and (14), the equality $F_2^A/F_2^D = \sigma^A/\sigma^D$ holds if $R^A = R^D$. Measurements of the structure function $R(x,Q^2)$ are less accurate and much more subject to systematic errors than measurements of $F_2(x,Q^2)$. The reason for this is the need to make the experiment at different energies of the incident lepton, and also the special procedure for extracting R. The most accurate values of $R(x,Q^2)$ in muon experiments on nuclei, averaged over the corresponding kinematic intervals, were obtained by the BCDMS,[40] EMC,[41,42] and Berkeley–FNAL–Princeton (BFP)[43] collaborations:

$$\begin{cases} R^C = 0.015 \pm 0.013_{stat} \pm 0.026_{syst} & \text{(BCDMS)}, \\ R^{Fe} = -0.06 \pm 0.06_{stat} \pm 0.11_{syst} & \text{(BFP)}, \\ R^{Fe} = 0.03 \pm 0.12 & \text{(EMC)}, \\ R^D = 0.00 \pm 0.10 & \text{(EMC)}. \end{cases} \tag{20}$$

It can be seen from this that in the region of the EMC experiment ($Q^2 > 9$ GeV^2) one can assume $R^A = R^D = 0$ with good accuracy, and, therefore, the ratio of the cross sections is equal to the ratio of the structure functions. In the region of smaller Q^2 values, in which the results of the measurements of the SLAC–MIT group[39] lie, $R^A \neq 0$, and there is a weak growth with increasing A, possibly in accordance with the law $R(A) = 0.08A^{1/3}$.

In Refs. 44 and 45, the ratios of the cross sections (19) were converted to ratios of the structure functions (4) with allowance for the values of R^A measured at SLAC and their possible growth with increasing A. It was shown that the differences existing in the measurements of R^A for deuterium and iron make it possible, within the errors, to reconcile the results of the measurement of $r^A(x)$ by the EMC and SLAC groups in the region $x < 0.3$. In Fig. 5, the original EMC effect is represented by the solid line. With allowance for the possible A dependence of R, it is transformed into the dotted curve, which agrees qualitatively and quantitatively with the SLAC–MIT measurements. These calculations demonstrated the importance of high-precision experiments to measure the A dependence of the structure function $R = \sigma_L/\sigma_T$, and such measurements were subsequently made at SLAC.[46]

Despite these considerations, the question of the behavior of the ratio of the structure functions at $x < 0.3$ remained open until the publication of the results of the BCDMS collaboration.[47] Because of the unique properties of the toroidal spectrometer[48] with distributed detectors and targets, which gave it an acceptance close to ~100% and weakly dependent on the kinematic variables, and also because of the high luminosity, the BCDMS collaboration could carry out an experiment in the same region of x and Q^2 as the EMC experiment, but with much lower statistical and systematic errors. A large proportion of the errors canceled because data were collected from two targets of different nuclear composition—nitrogen and iron or deuterium and iron—simultaneously (Fig. 6). In addition, the experiments with deuterium and nitrogen were made with completely identical geometry. As a result, the statistical and systematic errors of the ratios r^N and r^{Fe} were ap-

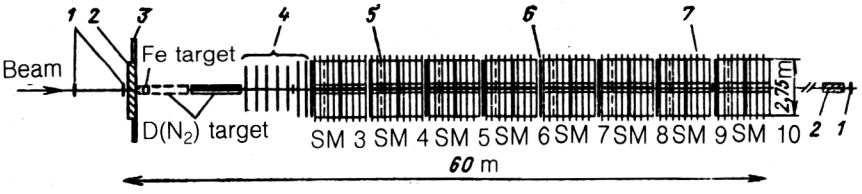

FIG. 6. Schematic form of spectrometer of the BCDMS collaboration used to investigate nuclear effects: *1*) beam hodoscopes; *2*) iron screen; *3*) anticoincidence counters; *4*) hexagonal multiwire proportional chambers; *5*) mosaic trigger counters (eight planes); *6*) fragmented trigger counters (16 planes); *7*) multiwire proportional chambers (64 planes).

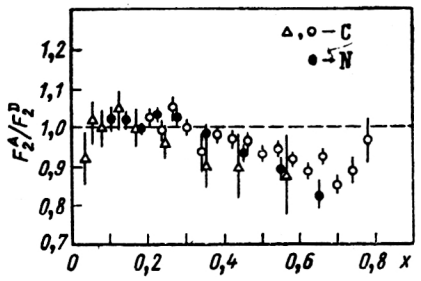

FIG. 7. Ratios of structure functions (black circles, Ref. 47; open triangles, Ref. 48) or cross sections (open circles, Ref. 39) as functions of x measured in the SLAC, BCDMS, and EMC experiments on light nuclei.

proximately the same, varying from 1 to 4% in individual intervals with respect to the variable x.

We consider separately the BCDMS results obtained on the light (N) and heavy (Fe) nuclei. The experiment on the nitrogen and deuterium targets was decisive for clarifying the behavior of $r^A(x)$ in the region $x < 0.3$.[47]

Figure 7 shows the ratios $r^N(x)$ averaged over the range $Q^2 = 26$–$200\ \text{GeV}^2$. Whereas for $x > 0.3$ these results can be regarded as one further confirmation of the effect discovered by the EMC collaboration, at smaller values of x there is a result that is qualitatively new for large Q^2: $r^N(x)$ is practically equal to unity. Later, the EMC collaboration confirmed, admittedly with poorer accuracy, this conclusion by new measurements on carbon and deuterium[48] (Fig. 7).

Significant differences from the original EMC results[10] were observed by the BCDMS collaboration[49] in the region $x < 0.3$ and in the x dependence of the ratio $r^{Fe}(x)$. These data are given in Fig. 8 together with results of the SLAC experiments on iron[39,46] and copper[50] nuclei. Instead of linear growth with decrease of x from 0.3 to 0.06, a "flattening" of $r^{Fe}(x)$ is observed, and at $x = 0.2$–0.06 we have $r^{Fe} = 1.054 \pm 0.005$. Qualitatively and quantitatively, this is confirmed by the data of Refs. 50 and 51. The results of the experiment of Ref. 39 discussed above also agree with such behavior, but at $x < 0.2$ they are systematically below the BCDMS results by 2–3%. In our opinion, this shift can be attributed to a less complete procedure for taking into

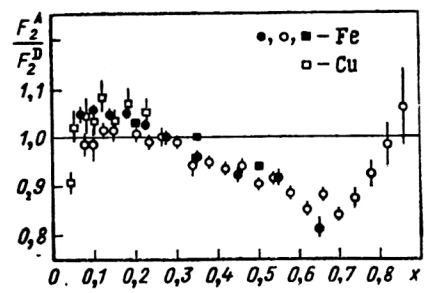

FIG. 8. Ratios of cross sections (black circles, Ref. 49; black squares, Ref. 46) or cross sections (open circles, Ref. 39; open squares, Ref. 50) obtained in the SLAC and BCDMS experiments on heavy nuclei.-

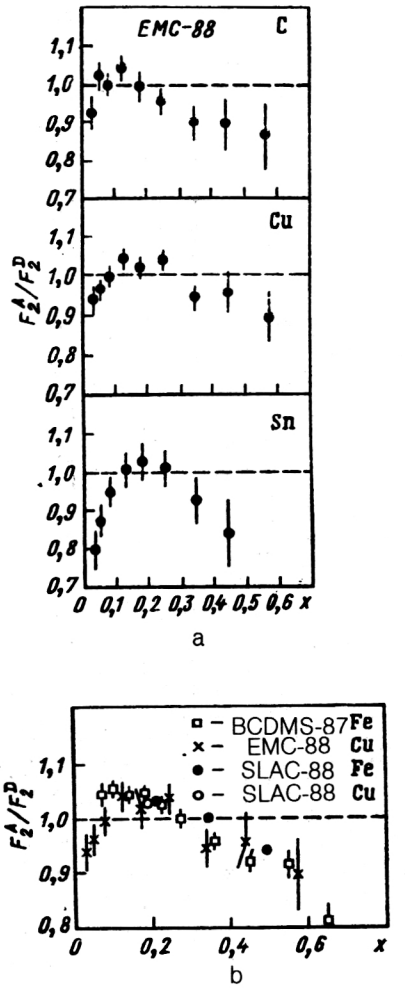

FIG. 9. Results of the second (1988) EMC experiment[48] obtained with significantly lower systematic errors than in the first experiment (Ref. 10) (a) and comparison of results of the EMC-88 experiment on a copper target with the high-precision BCDMS and SLAC experiments on copper and iron targets (b).

account radiative corrections used in Ref. 39 or underestimation of the systematic errors.

As we have already noted, at very small x ($x < 0.05$) it was expected that the ratio r^A could be less than 1.0, owing to effects of nucleon screening in a nucleus (see Fig. 8). The flattening of the ratios $r^A(x)$ at $x < 0.2$ also indicates a possible change of regime to $r^A(x) < 1$ at $x < 0.1$. All this was a motivation for new measurements of $r^A(x)$ at CERN. An experiment, some of the results of which have already been given in Fig. 7, was made by the EMC group.[48] Deuterium, carbon, copper, and tin were used as targets in it. Efforts were made to minimize the possible systematic errors by optimizing the target construction and frequent target replacement in the beam. This last procedure averaged the possible fluctuations of the beam phase space and instability of the apparatus. As a result, the systematic errors in the measurements of $r^A(x)$ in any interval of x did not exceed 2–3%. The results of the measurements are shown in Fig. 9a and demonstrate that in the region $x < 0.1$ the ratio $r^A(x)$ decreases with decreasing x

to 0.8–0.9. The decrease of $r^A(x)$ in this kinematic region becomes significantly more pronounced with increasing atomic mass of the target. Approximately this behavior of the ratio of the structure functions was expected in a model describing nucleon screening in nuclei in the framework of the parton picture.[28] In the region $x<0.1$ the data of this experiment agree with other data (see Figs. 7, 8, and 9b).

Whereas the nuclear effect discovered in the EMC experiment in the region of central values of x was unexpected, the screening of nuclear nucleons at $x=0$ was predicted and was well known through experiments on photoproduction on free nucleons and nuclei.[52] The essence of this phenomenon is a decrease in the cross section (per nucleon) for interaction of a real photon with a nucleus with increasing atomic mass of the nucleus. Possessing the properties of a hadron, the real photon is strongly absorbed by the nuclear medium, as a result of which the nucleons closer to the center of the nucleus are screened by the outer nucleons. A similar effect must be observed for the interaction of virtual photons with a nuclear medium as long as the squared 4-momentum transfer is small and does not exceed $Q^2 \sim 1\ \text{GeV}^2$. A weakening of the screening with increasing Q^2 is predicted by the vector-dominance model.[53] A screening independent of the mass of the virtual photon is also predicted in the quark–parton model.[28] In this approach, partons belonging to different nuclear nucleons are expected to become united at small x. The corresponding region is determined by

$$x<x_c A^{1/3}, \tag{21}$$

where $x_c \sim m_\pi/M \approx 0.15$.

The redistribution of the parton momenta in the nucleus must lead to antiscreening, i.e., to a growth of the ratio $r^A(x)$ at $x \gtrsim 0.1$. To make a detailed study of nuclear effects at small x, measurements were made at CERN of the nucleon structure functions by means of deep inelastic scattering of 280-GeV muons by deuterium, carbon, and calcium nuclei.[54] A special trigger realized by means of scintillation hodoscopes and rapid processors made it possible to select events with emission angle of the scattered muon beginning at 2 mrad, and this made it possible to obtain data in the region $0.003<x<0.1$ and $0.3 < Q^2 < 3.2\ \text{GeV}^2$.

The results of this experiment, represented in the form of the structure-function ratios F_2^A/F_2^D, are given in Fig. 10. For comparison, the results of other experiments in the region $x>0.1$ are also given. The stronger rise of $r^A(x)$ with increasing x on the calcium nucleus confirms the conclusions of Ref. 48 (see Fig. 9a) regarding an enhancement of the screening with increasing mass number of the nucleus. Dividing the measured data into two groups—up to $Q^2 = 1\ \text{GeV}^2$ and above—the authors showed that screening is manifested equally in the two intervals of Q^2. This is a strong indication that the screening mechanism proposed in the vector-dominance model does not describe the nuclear effects observed in this experiment. At the same time, the persistence of this effect with increasing Q^2 supports the parton interaction picture.

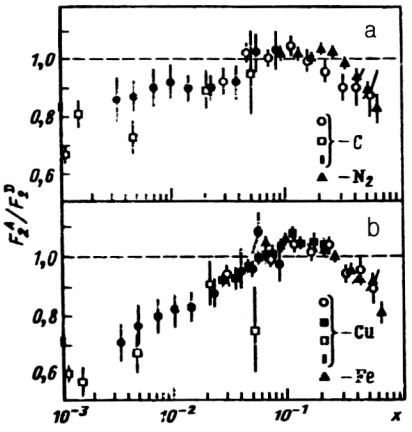

FIG. 10. Results of investigation of screening effects in the region $x<0.1$ obtained in EMC experiments[54] on carbon (a) and calcium (b) (black circles). For comparison, the results of other experiments are given: open circles, Ref. 48; black squares, Ref. 50; black triangles, Refs. 47 and 49; open squares, Ref. 84; vertical rods, Ref. 52.

More detailed information about nuclear effects in the region of small x is expected from the experiment made at Fermilab by the E665 collaboration.[55] The spectrometer used in this experiment makes it possible to detect events with deep inelastic scattering of muons by nuclei in the kinematic intervals $x\in(0.001,\ 0.08)$ and $Q^2\in(0.1,\ 10\ \text{GeV}^2)$. Preliminary data obtained for the ratio of the cross sections for scattering on xenon and deuterium nuclei indicate an absence of a Q^2 dependence of r^A in this region. It has also been confirmed that the screening effect is enhanced with decreasing x: r^A decreases to 0.62 at $x = 0.002$.

Besides the experiments to investigate the EMC effect in the reactions (5) and (6), attempts were made to measure the ratio $r^A(x)$ by means of the neutrino and antineutrino deep inelastic reactions (7) and (8) on nuclei. Despite the poorer accuracy than in experiments on electron and muon scattering, the neutrino experiments do have some qualitative advantages over them.

First, as can be seen from the diagram in Fig. 1b and from Eqs. (13a) and (13b), neutrinos and antineutrinos interact differently with quarks and antiquarks. For example, in the limit $y\to 1.0$ the contribution of the quark distributions is dominant in the interaction cross section, whereas it is the contribution of the antiquarks (the so-called sea quarks) that is dominant in the antineutrino interaction cross section. This gives the possibility of comparing the contributions of the sea quarks to the structure functions of free and bound nucleons.

Second, the data of the neutrino experiments cover a wider range in Q^2 than the electron and muon scattering experiments at the same values of x. This permits study of the Q^2 dependence of the EMC effect at small values of x, as is needed for a detailed study of the screening effects.

In neutrino experiments, r^A can be calculated by means of the combination of cross sections

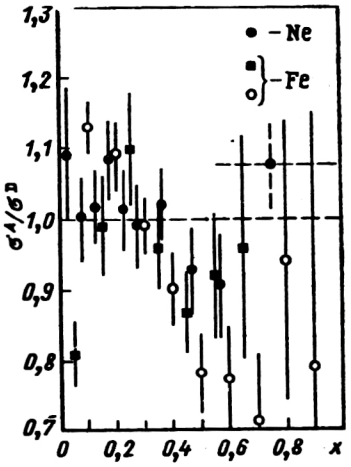

FIG. 11. Ratios of cross sections measured on nuclei in the most accurate neutrino experiments: black circles, Ref. 56; open circles, Ref. 58; black squares, Ref. 57.

$$r^A(x) = \frac{d\sigma_\nu^A + d\sigma_{\bar\nu}^A}{d\sigma_\nu^D + d\sigma_{\bar\nu}^D}, \tag{22}$$

which is proportional to the quark singlet distribution $\Sigma(x)$ [see (13a) and (13b)]. The values $r^A(x)$ obtained in the experiments of Refs. 56–58 are given in Fig. 11. The statistical accuracy of even the most accurate of the neutrino experiments, WA25–WA59 (Ref. 56), is significantly inferior to that of the experiments in the muon and electron beams. However, these data do not contradict the main features of the $r^A(x)$ behavior established in beams of charged leptons. If the results of measurement of r^A in the experiment of Ref. 56 in the region of x from 0.2 to 0.6 are described by a linear dependence, then the slope is

$$b = -0.33 \pm 0.18, \tag{23}$$

in agreement with the values of the parameter b given in Table I.

It can also be seen from Fig. 11 that the neutrino data did not contradict the flattening of $r^A(x)$ at $x < 0.2$, the change of regime at $x < 0.1$, the presence of a minimum of $r^A(x)$ at $x \sim 0.7$, and the other features of the EMC effect established with better accuracy by means of muons and electrons.

We discuss separately the attempts to establish the nature of the EMC effect by using the properties of weak interactions. In Ref. 56, a comparison was made of the cross sections for antineutrino scattering by deuterium (WA25 collaboration) and neon (WA59 collaboration) filling the BEBC bubble chamber at CERN. As we have already noted, scattering by sea quarks is dominant in these cross sections under certain conditions. Although these data were obtained in two different experiments, the authors were able to ensure selection of events in an overlapping region of two reference spaces in the chamber, and also to show that these events were obtained under identical conditions of irradiation with the antineutrino beam. These and also some other measures adopted in the data analysis helped to lower the systematic errors. As a result, it was possible to demonstrate that for $x < 0.2$ the contribution of the sea quarks to the structure function of the heavy nucleus did not exceed their contribution to the structure function of the deuterium nucleus. A similar result was obtained[57] for the iron and hydrogen nuclei.

In Ref. 59, an interesting attempt was made to establish whether the structure of protons or neutrons is more sensitive to the influence of the nuclear medium. The "tag" for determining the reaction type,

$$\bar\nu + n \to \mu^+ + X^- \tag{24}$$

or

$$\bar\nu + p \to \mu^+ + X^0,$$

on a free or bound nucleon was the total charge of the final hadronic state. Data from a neon-filled 15-foot bubble chamber at Fermilab were selected and compared with data obtained from a deuterium-filled BEBC bubble chamber.[60] The results of the comparison indicate that at $x < 0.25$ the neutron structure function is changed more strongly in nuclei than the proton function. However, in view of the possible systematic errors this conclusion requires further confirmation.

One further original approach to study of the EMC effect was proposed in Ref. 61. The idea was to separate events from the reaction (7) into two groups, the first containing predominantly neutrino interactions on quasi-free nucleons belonging to the nuclear surface, and the second interactions with "well-bound" nucleons within the nucleus. According to the expectation of the authors, the events of the second group should differ from those of the first in photographs of events in the bubble chamber by the presence of dark tracks formed by protons emitted from the nucleus that on their path to the surface of the nucleus had lost energy through interaction with other nucleons.

This experiment was made at Fermilab using the 1.4-m hybrid bubble chamber Tohogu filled with freon. Interactions were detected by means of both traditional photographs and holograms. In principle, the latter permit selection of events with dark tracks whose minimal length is 0.5 mm. However, to speed up the analysis, a restriction was made to scanning of the photographs, in which dark tracks with length greater than 4 mm could be identified, corresponding to a minimal nucleon momentum $p_{\min} \approx 0.17$ GeV. Altogether, 553 events without dark tracks and 532 events with one or more dark tracks were selected. Figure 12 gives the results of comparison of the $\sigma^A(x)$ values obtained in this manner with the neutrino–deuterium deep inelastic scattering cross sections of Ref. 62. The comparison was made after normalization of the data of both experiments in the region $x > 0.1$. It can be seen from the figure that the x dependence of the ratio $r^A(x)$ characteristic of the EMC effect is more strongly manifested for the group of events with dark tracks. From the point of view of the idea of the experiment, this means that the structure of a nucleon is distorted more strongly the further it is from the surface of the nucleus.

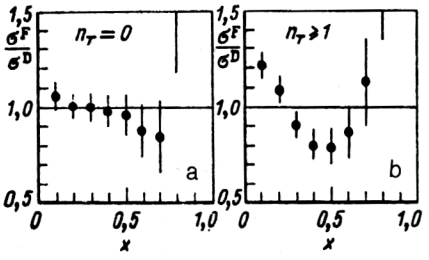

FIG. 12. Effect of variation of r^A measured in deep inelastic scattering of neutrinos by nuclei[61] as a function of the event selection criteria based on the appearance of the tracks of the secondary particles: a) events without dark tracks ($n_T = 0$); b) events with one or more dark secondary tracks ($n_T \geqslant 1$).

Dependence of nuclear effects on the 4-momentum transfer

As the experiments on the deep inelastic scattering of leptons by nucleons and nuclei showed, the structure functions of the nucleons change little with variation of Q^2 (Ref. 23). The scale of the variations is well illustrated by the phenomenological dependence used, for example, by the BCDMS collaboration to approximate the results of measurement of the structure functions on a carbon target:[40]

$$F_2(x,Q^2) = (1-x)^a(b + cx + dx^2 + ex^3)Q^{2(f+gx)}, \quad (25)$$

where $f = -0.0303$, $g = -0.2185$.

As we already noted in Sec. 2, the experiments showed that the partons constituting the nucleon are quarks—particles with fractional electric charges interacting with one another through the emission and absorption of gluons. It is the emission of gluons that leads to the small deviations from (violations of) scaling in the structure functions, which can be well described by QCD.[22] Since in the framework of QCD the Q^2 dependences of the structure functions of free nucleons and of nucleons bound in a nucleus must be the same, their ratio r^A must be independent of Q^2.

However, in the general case lepton scattering cannot be regarded merely as scattering by an isolated quark. The presence within the nucleon of the gluon field may lead to an influence on this process of the fields of the other quarks. Moreover, even weak effects of interaction with two quarks can be enhanced by their interference with scattering on one quark. As was shown in Ref. 64, effects of this type must lead to power-law[65] violations of scaling, and not the logarithmic violations predicted by QCD. The power-law $1/Q^2$ corrections to the logarithmic description of scaling violation are usually called the higher-twist (HT) corrections, and the nucleon structure function can be represented by means of them in the form

$$F_2(x,Q^2) = F_2^{\mathrm{LT}}(x, \ln Q^2) + F_2^{\mathrm{HT}}(x,Q^2) + \ldots,$$

where F_2^{LT} denotes the contribution of the leading twist, which has only a logarithmic dependence on Q^2. Calculations of the first power-law correction to $F_2(x,Q^2)$ show[65] that for $Q^2 = 40$ GeV^2 the higher-twist contribution increases from 1% at $x = 0.4$ to 10% at $x = 0.8$. Although the state of the theory of the higher twists is unsatisfactory (there are free parameters whose connection with the fundamental QCD parameter Λ is still unknown[65,67]), it is natural to expect that the presence of the nuclear medium will tend to increase the higher twists compared with the calculations for free nucleons.[68] Increase of the contribution of the higher twists to lepton deep inelastic scattering by nuclei must be indicated by the appearance of a Q^2 dependence of the nuclear effects in the structure functions. Thus, the contribution of the higher twists to $F_2^A(x,Q^2)$ can be revealed by investigating the structure functions F_2^N and F_2^A and their ratio in a wide range of the variable Q^2.

In the structure functions $F_2^A(x,Q^2)$, the nuclear effects could be manifested, for example, by approximating the experimental data by the corresponding expressions of perturbative QCD. Then if there is an important contribution of the higher twists to F_2^A, a poor agreement between theory and experiment must be expected, i.e., $\overline{\chi^2}/\chi^2 \gg 1$, and there should be an improvement after phenomenological addition of higher-twist terms. Possible "traces" of the higher twists were indeed found in this way in a number of experiments on lepton deep inelastic scattering (see, for example, the review of Ref. 23) in which there was overlapping of the region of comparatively small $Q^2 < 10$ GeV^2. In the most accurate BCDMS experiments at $Q^2 > 25$ GeV^2, $\chi^2/\overline{\chi^2} \simeq 1$ and the presence of higher twists in F_2 is not noted.[40] However, these data do not exhaust the question of the higher twists, which remains topical, particularly in the region of transition to QCD: $Q^2 = 1$–10 GeV^2.

One further way of observing a possible Q^2-dependent contribution of nuclear effects in $F_2^A(x,Q^2)$ consists of comparing the real violation of scaling with what is predicted by QCD. The prediction is that for a given parameter Λ the logarithmic slopes $b(x) = d \ln F_2/d \ln Q^2$ are a specific function of x determined by the quark composition of the target. Differences between the observed and predicted slopes $b(x)$ for the nucleon and nuclear F_2 could indicate a distortion of the structure functions by the medium. Such comparisons require a high accuracy of the measurements and were first made by the BCDMS collaboration. The QCD analysis of the hydrogen and carbon structure functions[69] showed (Fig. 13) that the violation of scaling in them agrees with the QCD predictions for the same parameter $\Lambda_{\overline{\mathrm{MS}}} = 220$ MeV and does not exhibit other Q^2-dependent nuclear effects.

Observation of a Q^2 dependence of the nuclear effects in the structure-function ratios is a problem no less difficult than in the structure functions themselves. The first EMC[10] and SLAC[39] experiments did not have the accuracy necessary for this. The problem of a Q^2 dependence was specially studied in BCDMS[47,49] and EMC[29] experiments in the region from 10 to 200 GeV^2, and also in neutrino experiments[56] in the region from 1 to 30 GeV^2. The ratios of the structure functions $r^A(Q^2)$ obtained in the experiments of the BCDMS group on nitrogen and iron targets

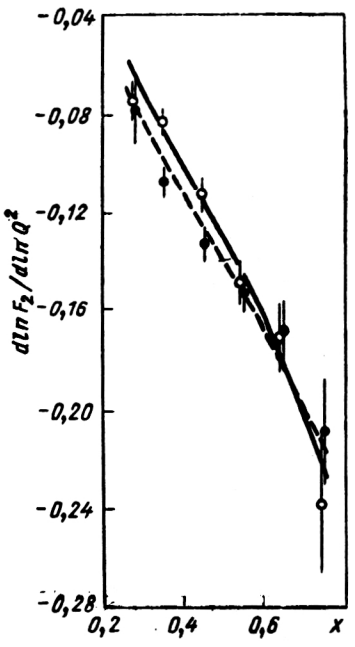

FIG. 13. Logarithmic derivatives $d \ln F_2(x,Q^2)/d \ln Q^2$ determined from the results of the BCDMS experiments on carbon (black circles) and hydrogen (open circles). The QCD prediction for carbon (broken curve) and hydrogen (continuous curve) was obtained for the parameter $\Lambda_{\overline{MS}} = 220$ MeV.

(Fig. 14a) demonstrate that within the errors

$$r^A(Q^2) = \text{const.}$$

The same conclusion follows from the experiment of Ref. 56, though admittedly for smaller intervals, chosen thus by virtue of low statistics (Fig. 14b).

Thus, within the kinematic interval of each of the experiments a Q^2 dependence of the nuclear effects in the ratios of the structure functions was not observed. Because of the importance of this question, attempts were made[63] to extend the range of measurements with respect to Q^2 and analyze together the BCDMS and SLAC data, i.e., the data of the two experiments in which the systematic errors were minimal. To this end, the ratio $r^A(x,Q^2)$ was represented in each interval of x in the form

$$r^A(Q^2) = r^A(Q_0^2) + r' \ln \frac{Q^2}{Q_0^2}, \tag{26}$$

where

$$r' = \frac{dr^A(Q^2)}{d \ln Q^2}$$

The values of the derivative r' obtained as a result of the fit are shown in Fig. 14c, which gives only the statistical errors. It can be seen that there is a slight deviation of r' from zero at $x > 0.4$, i.e., in the region in which manifestation of the higher twists is expected. However, in view of the possible systematic errors of the two experiments, it may be assumed that in this region too, $r' \approx 0$. Thus, to establish a possible weak Q^2 dependence of the ratio $r^A(x,Q^2)$ a further increase in the accuracy of the experiments is required.[70,71] In particular, progress is expected from the experiments currently being made at CERN by the New Muon Collaboration.[72]

Dependence of nuclear effects on atomic mass

The experiments described above convincingly demonstrated a change in the quark structure of a nucleon in a nuclear medium compared with the structure of the free nucleon. It was natural to expect a dependence on the atomic mass A of characteristics of the observed effect. The most complete investigations of the EMC effect with different targets were made using the SLAC electron beam.[39] A deuterium target and eight other targets in a wide range of atomic masses were chosen: He, Be, C, Al, Ca, Fe, Ag, and Au. Figure 4 shows results obtained in these experiments for the cross-section ratios integrated over the range of variation of the variable Q^2 from 2 to 10 GeV^2. In these experiments, the structure functions $R = \sigma_L/\sigma_T$ were not measured, and, therefore, there was no possibility of representing the results in terms of the ratios (4). However, experiments made subsequently[51] showed that $R(x)$ does not depend on the species of the nucleus for $x > 0.3$, and, therefore, in this region the ratio of the cross sections is equal to the ratio of the structure functions. This fact was tacitly extended to the entire range of measurements with respect to x.

As can be seen from Fig. 4, the picture of the x dependence of the ratio r^A characteristic of the EMC effect remains the same for all nuclear targets from helium to gold. It can also be seen that for a fixed value of x the ratio r^A is practically independent of A in the region $x \approx 0.2$–0.4 but does change quite strongly with increasing A in the region $x \approx 0.5$–0.7, indicating an enhancement of nuclear effects for heavy nuclei (Fig. 15). Besides the results of Ref. 39, Figs. 15a and 15b give BCDMS and EMC results, which agree with them, and also the approximation of the distortion of the nucleon structure function in the nuclear medium with increasing A by the simple dependence

$$r^A(x) = cA^{\alpha(x)}. \tag{27}$$

The values of $\alpha(x)$ for all x are given in Fig. 15c.

As can be seen from these data, the nature of the A dependence of r^A is too weak to expect appreciable distortions of the structure function of the lightest nucleus, deuterium, compared with the structure function of the free nucleon. It is also known that the internuclear separation for the deuterium nucleus is about 4 fm, which is appreciably greater than the separation (about 1 fm) characteristic of heavy nuclei. Taking into account the short range of the nuclear forces, it is natural to propose that the nucleons in the deuterium nucleus are not subject to the effects that are observed in the heavy nuclei and that the structure functions of the nucleons in the deuterium nucleus are identical to those of the free nucleon. Experimental verification of this is made difficult by the absence of neutron targets.

However, there are arguments which suggest that the deuterium nucleus, despite its "fragility," must also intro-

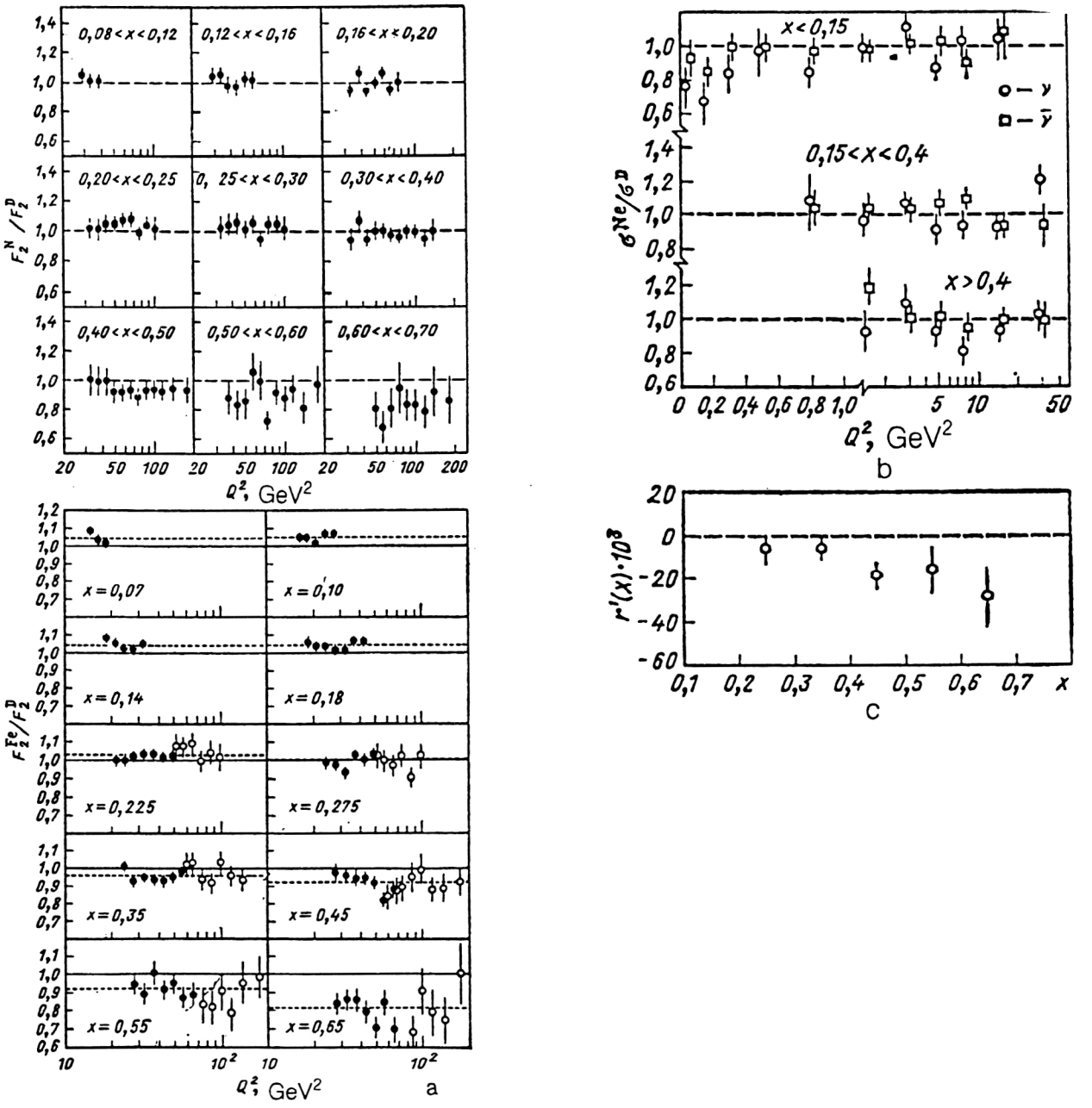

FIG. 14. Dependence of r^A on Q^2: a) obtained by averaging F_2^A/F_2^D in narrow intervals of x (from the BCDMS experiments on deep inelastic scattering of muons); b) by averaging σ^{Ne}/σ^D in wide intervals of x (from experiments on deep inelastic scattering of neutrinos); c) by calculation of the slope parameter r' of the logarithmic dependence of r^A on Q^2 for the given interval of x (from the SLAC and BCDMS experiments). The broken lines show the mean value of F_2^{Fe}/F_2^D (BCDMS) for each x interval. Similar dependences were obtained in the EMC experiment[29] on iron.

duce distortions into the nucleon structure. For example, in Ref. 73 it is assumed that the deviation of r^A from unity must be proportional to the density of nucleons in the nucleus. Comparing then the density of the nucleons in the iron and deuterium nuclei, the authors conclude that the EMC effect in the deuterium nucleus is about five times weaker than in the iron nucleus:

$$\frac{r^D(x=0.5,Q^2)-1}{r^{Fe}(x=0.5,Q^2)-1}\sim\frac{1}{5}. \tag{28}$$

In principle, the deuteron structure function $F_2^D(x)$ can be calculated with much higher accuracy than the structure function $F_2^A(x)$. This is true because a high accuracy has now been achieved in the description of the deuteron wave function,[74] and the structure function of a nucleon in a deuterium nucleus can be calculated in a self-consistent approach. An attempt at such a calculation was made in Ref. 75 in the framework of the impulse approximation, modified by inclusion of the effect of coupling of the nucleons in the deuterium nucleus by means of meson exchange currents. According to the results, the maximal deviations of the deuteron structure function from the structure function of the free nucleon in the region of central values of x are 1.5%.

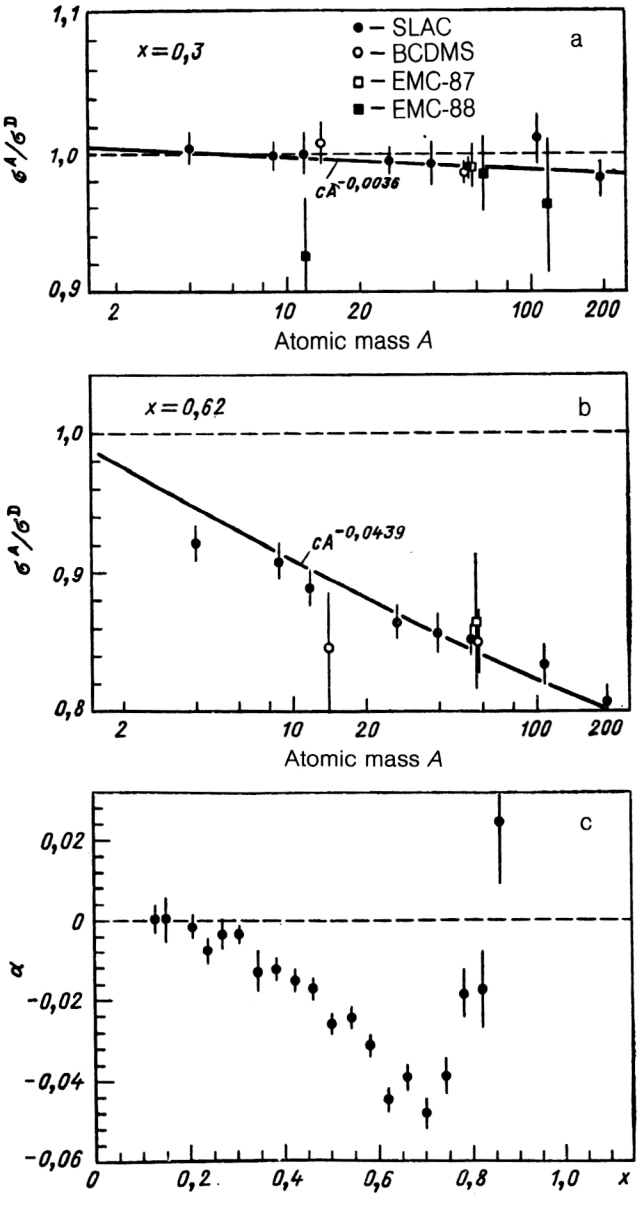

FIG. 15. Dependence of ratios of cross sections (SLAC) and structure functions (BCDMS and EMC) on the atomic mass A for $x = 0.3$ (a) and $x = 0.62$ (b) and values of the parameter $\alpha(x)$ of the fit to the SLAC results in the form $r^A = cA^\alpha$ (c). The result of the $r^A(x)$ fit is shown by the continuous line (Figs. 15a and 15b)

The interest in this question is strengthened in connection with searches for an understanding of the analogy that may exist between the confinement effect and the EMC effect. In this case, as is shown, for example, in the color dielectric model,[76] the nuclear effects in the deuteron may be large. In this connection,[77] an analysis was made of experimental data on deep inelastic scattering of electrons by protons and deuterons with the aim of determining the ratio

$$r^D(x) = \frac{F_2^{ed}}{(F_2^{ep} + F_2^{en})_{\text{free}}}. \tag{29}$$

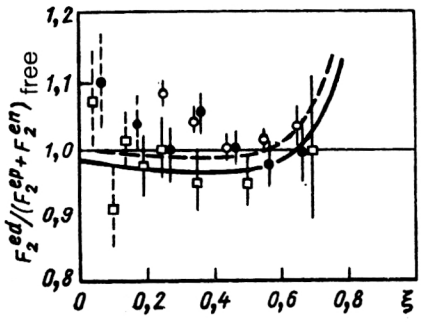

FIG. 16. Ratio of deuteron structure function to the sum of the neutron and proton structure functions in its dependence on the scaled variable ξ.[77] The errors in the data in the region $\xi < 0.2$ do not take into account the additional uncertainty in the violation of scaling and are shown by the broken vertical lines. The values of d/u needed to calculate the ratios (31) and (32) were obtained in different neutrino experiments: black circles, CDHS; open circles, BEBC (WA21); open squares, BEBC–TST. The calculations were made with allowance for only Fermi motion of the nucleon, shown by the continuous curve (Atwood–West) and broken curve (Frankfurt–Strikman).[30]

In order to overcome the difficulty associated with a determination of F_2^{en} free of nuclear effects, the authors used the quark–parton model, which makes it possible to express the structure-function ratio F_2^{en}/F_2^{ep} in terms of the ratios of the distributions of the valence u and d quarks measured in neutrino experiments:

$$r^D(x) = \frac{F_2^{ed}}{F_2^{ep}(1 + F_2^{en}/F_2^{ep})}, \tag{30}$$

$$\frac{F_2^{en}}{F_2^{ep}} = \frac{1 + 4d/u}{4 + d/u} \tag{31}$$

The expression (31) is valid in the region $x > 0.3$, where one can ignore the contribution of the sea quarks to the nucleon structure function. In the region $x < 0.3$, where this contribution cannot be ignored, the authors used the relation

$$\frac{F_2^{en}}{F_2^{ep}} = \frac{1 + 4d/u + (\bar{u} + 4\bar{d} + 2\bar{s})/u}{4 + d/u + (4\bar{u} + \bar{d} + 2\bar{s})/u} \tag{32}$$

and the following assumption about the relation between the sea quarks:

$$\bar{u} = \bar{d} = 2\bar{s}. \tag{33}$$

The results of this analysis are shown in Fig. 16 as functions of the variable $\xi = 2x/[1 + (1 + 4M^2x^2/Q^2)^{1/2}]$. The errors for the points lying below $x = 0.3$ are shown by the broken lines in order to emphasize that the calculations of them are less reliable than for the region $x > 0.3$. As can be seen from Fig. 16, the deuterium nucleus does not introduce distortions into the structure function of the free nucleon—the calculated ratio (30) is equal to 1.0 even in the region $0.5 < x < 0.7$, where for heavy nuclei the maximal deviation of r^A from unity is observed.

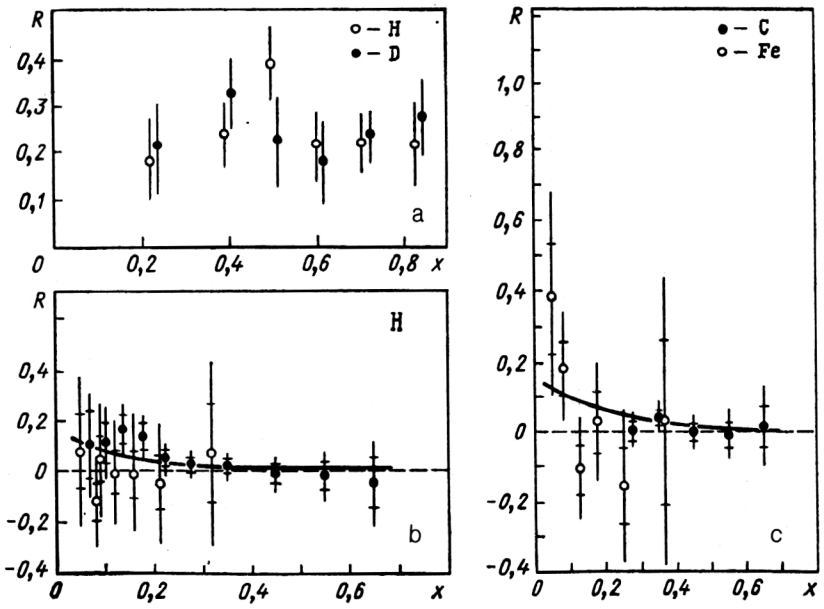

FIG. 17. Dependence of the structure function $R = \sigma_L/\sigma_T$ on x: a) $Q^2 < 18$ GeV^2, SLAC; b) and c) $Q^2 > 12$ GeV^2 from BCDMS (black circles) and EMC (open circles) experiments on hydrogen (b) and on heavy nuclei (c).

Nuclear effects in the structure function $R(x,Q^2) = \sigma_L/\sigma_T$

As we noted above, reliable information about the structure-function ratio F_2^A/F_2^D can be obtained in the cases when there exist high-precision measurements of the structure functions $R = \sigma_L/\sigma_T$ on heavy nuclei and the deuterium nucleus, or when the value of the structure function R does not depend on the atomic mass of the nucleus, or if $R = 0$. The experimental difficulties and importance of measurements of R for different targets have already been discussed.

The most accurate values of $R(x)$ on light and heavy nuclei are given in Fig. 17. The main difference between the experiments made at SLAC[33] (Fig. 17a) and CERN[40–42,68] (Figs. 17b and 17c) is that the measurements covered different kinematic regions. The SLAC results were obtained at $Q^2 < 18$ GeV^2, and the CERN results at $Q^2 > 12$ GeV^2. The data show that in the region of large values of Q^2 the structure functions R are small and therefore have little influence on the observed cross sections. In contrast, $R > 0.2$ in the region of small Q^2, and investigation of the nuclear effects in the structure function $F_2(x,Q^2)$ is impossible without high-precision measurements of the structure functions R, especially[45] for the region of small $x(x < 0.3)$. The nature of the decrease of $R(Q^2)$ with increasing Q^2 can be clearly seen in Fig. 18, which gives the results of experiments on deep inelastic scattering of electrons by nuclei[78] (SLAC) and of muons by carbon[40] (CERN). At SLAC, an investigation was also made of the A dependence of the structure function R in experiments with deuterium, iron, and gold targets.[51] The results are represented in the form of the difference $R^A - R^D$ of the structure functions in its dependence on the variable x, and they are given in Fig. 19. Because the spectrometer for the scattered electrons used in this experiment had a small acceptance, it was not possible to obtain data on the structure functions R at $x < 0.2$, where the possible deviations of R^A from R^D are most important for the study of $r^A(x)$. Within the experimental errors, which were $\Delta R \approx 0.1$, the results in Fig. 19 support equality of the structure functions $R = \sigma_L/\sigma_T$ measured on heavy nuclei and deuterium at $x > 0.2$.

Although the neutrino experiments are inferior to the muon and electron experiments in statistics, they do have the advantage of ensuring a more uniform acceptance in the region of small values of the variable x, and also a uniform acceptance in the complete range of the variable $y = \nu/E$. This last circumstance was exploited in Ref. 56 to study the influence of nuclear effects on the structure function R by comparing the cross sections for deep inelastic scattering of neutrinos and antineutrinos by neon and deu-

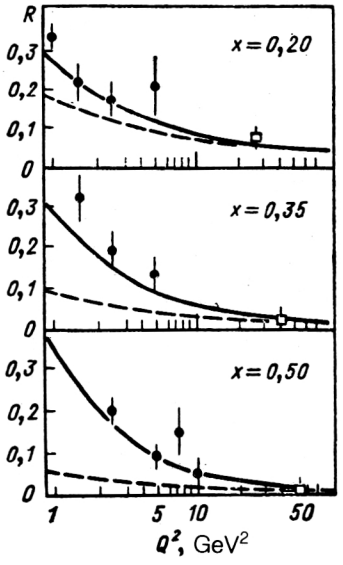

FIG. 18. Dependence on Q^2 of the structure function $R = \sigma_L/\sigma_T$ obtained by averaging the results of SLAC measurements on deuterium, gold, and iron nuclei (black circles) and BCDMS measurements on carbon (open squares). The QCD predictions are shown with allowance for the corrections for the target mass (continuous curves) and without allowance for the corrections (broken curves).

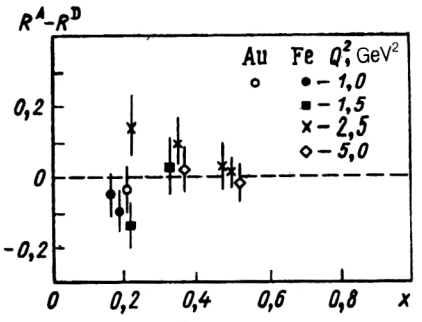

FIG. 19. Difference of structure functions $R^A - R^D$ measured in the SLAC experiment[51] on heavy nuclei (gold, iron) for some values of the mean 4-momentum transfer.

terium targets. As follows from Eqs. (11) and (14), the growth of the structure function $R = \sigma_L/\sigma_T$ for the heavy nucleus compared with that of the deuterium nucleus leads to a decrease of the ratio of their cross sections with increase of the variable y. The results of the measurements in Fig. 20 can be used to estimate possible variations of the structure function R under the influence of the nuclear medium. If it is assumed that these variations are described by a linear dependence $R = a + by$, then the slope is $b = 0.06 \pm 0.08$. Thus, within the errors of the experiment it can be assumed that the nuclear medium does not distort the values of the structure function $R = \sigma_L/\sigma_T$.

Structure function of carbon near $x=1.0$

The experiments considered hitherto were restricted to study of nuclear effects in the structure functions in the region $x<0.9$. The value $x = 1.0$ corresponds to the kinematic limit for the case of lepton scattering by a nucleon at rest. Because for a free nucleon $F_2^N(x)|_{x\to 1} \to 0$, the relative fraction of nuclear effects in F_2^N must increase as the kinematic limit is approached. The tendency for $r^A(x)$ to increase as $x \to 1.0$ can be clearly seen in Figs. 3 and 4, from which it follows that at $x = 1.0$ the ratio $r^A(x)$ of the structure functions of heavy nuclei and the deuterium nucleus can reach values $r^A \approx 2$–3. If, in addition, it is borne in mind that as a consequence of the nuclear effects F_2^N in the limit $x \to 1.0$ can exceed the structure function of the free nucleon by several times, then we conclude that in this

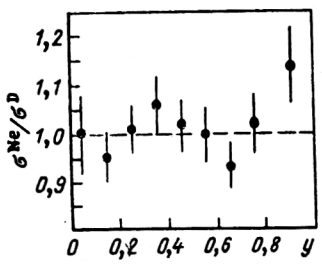

FIG. 20. Ratio of cross sections for deep inelastic scattering of neutrinos and antineutrinos by neon and deuterium nuclei as a function of the variable y (Ref. 56) for events with $Q^2 > 1$ GeV^2.

region $F_2^A \gg F_2^N$. Thus, near the kinematic limit we have grounds for speaking of F_2^A as the nuclear structure function.

It is obvious that experiments to measure F_2^A in the region $x > 1.0$ can give important quantitative information about the quark–parton structure of nuclei. However, as this boundary is approached, and beyond it, the experimental difficulties increase appreciably. The reason for this is, first, that the measured cross sections are here 3–4 orders of magnitude lower than in the region of central values of x and, second, that the decrease in the resolution of the experimental facilities with respect to the variable x and the rapid change of F_2^A lead to appreciable smearing of the spectra of the events detected in an experiment.

Up to now, these difficulties have not been overcome in the region $x > 1.2$. The results of measurements of F_2^A in experiments on a carbon (BCDMS collaboration)[79] and an iron (CDHSW collaboration)[80] target should be regarded as giving an upper estimate of the nuclear structure function for $x > 1.2$. In the region $x < 1.2$, the BCDMS collaboration measured the structure function $F_2^C(x,Q^2)$ of the carbon nucleus at squared 4-momentum transfers Q^2 equal to 61, 85, and 150 GeV^2 (Ref. 81). As we have already noted, the BCDMS spectrometer has a high efficiency, permitting investigation of muon deep inelastic scattering near $x = 1.0$. With regard to the problem of recovering the smeared spectrum of the scattered muons, it was solved in Ref. 81 by analysis of data obtained under the same conditions with a hydrogen target.

The results of the determination of F_2^C are given in Fig. 21 together with theoretical calculations[82] in the framework of a model of few-nucleon correlations. The deformation of the wave function of the bound nucleon was described in Ref. 82 by the introduction of a factor δ, which was represented by two different expressions. Besides this, calculations were made for two values of the parameter ΔE_A, which describes the excitation energy of a nucleon within the nucleus: $\Delta E_A = 0.7$ GeV and $\Delta E_A = 0.9$ GeV. Because of this, the predictions of the model for F_2^C cover a wide strip, the lower boundary of which agrees satisfactorily with the experimental results.

The results of the experiment of Ref. 81 also agree with the predictions of Ref. 83 for F_2^C at $Q^2 = 60$ GeV^2 in the framework of a model that represents F_2^C as a sum of the structure function of a free nucleon and a multiquark cluster. The parameters of the model were obtained by fitting the results of the SLAC experiment[39] at $x \leqslant 0.8$.

As can be seen from Fig. 21, the value of the structure function of the carbon nucleus at $x = 1.0$ is $(1.1$–$1.3) \times 10^{-4}$, and its x dependence in the neighborhood of this point can be approximated by an exponential:

$$F_2^C(x) \sim \exp(-sx).$$

The results of the fit give $s \approx 16$, practically independently of Q^2. For $Q^2 = 150$ GeV^2, $s = 15.6 \pm {}^{0.8}_{0.6}$. The error given here includes the statistical and systematic errors.

Summarizing all the experimental data considered in this section, we may note that the x dependence of the ratio $r^A(x) = F_2^A(x)/F_2^D(x)$ of the structure functions of nu-

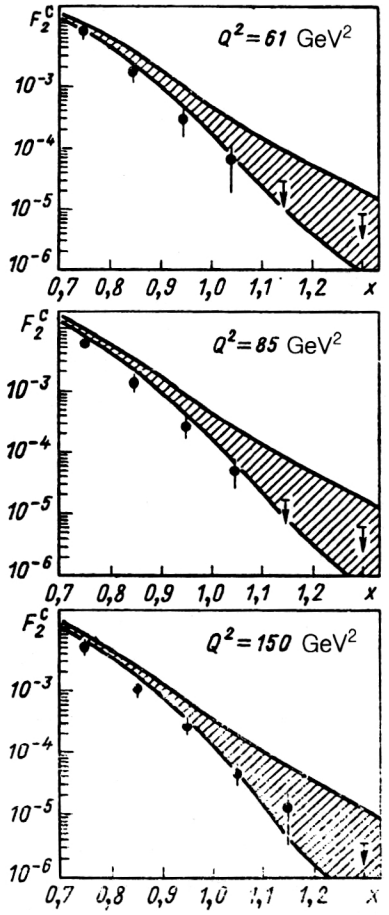

FIG. 21. Structure function $F_2^C(x)$ of the carbon nucleus.[81] The hatched regions correspond to the theoretical predictions.[82]

cleons bound in a nucleus and in the free state, or of the ratio $r^A(x) = \sigma^A/\sigma^D$ of the cross sections for deep inelastic scattering of leptons by the nuclei A and D, has the features shown schematically in Fig. 22: 1) at three points, $x_1 \sim 0.07$, $x_2 \sim 0.3$, and $x_3 \sim 0.8$, the ratio r^A is equal to unity; 2) in the interval $0 < x < x_1$ the ratio is $r^A(x) < 1.0$, with $r^A \sim 0.7$–0.9, and its deviation from unity is larger, the greater the atomic mass A; 3) in the interval $x_1 < x < x_2$, $r^A(x) \gtrsim 1.0$, and the small excess (2–4%) over unity appears to be proportional to A and increases with A; 4) in the interval $x_2 < x < x_3$, $r^A(x) < 1.0$, and there is a clear minimum ($r^A \approx 0.8$) at $x \approx 0.65$; 5) in the interval $x_3 < x < 1.0$, $r^A(x) > 1.0$. The asymptotic behavior of $r^A(x)$ as $x \to 1.0$ has not been studied because of the scarcity of data in this region.

5. REACTIONS ON NUCLEONS BOUND IN A NUCLEUS

Inclusive pion production

In accordance with Ref. 11, the existence of scaling in both lepton–nucleon and hadron–hadron collisions indicates the possibility of fusion of the nucleons of a nucleus into a "droplet." This may occur either through a fluctuation of the density of the nuclear matter,[4)] or as a result of the interaction of a nucleus with a target. In the parton language, the fusion of nucleons into a droplet means that the partons belonging to the individual nucleons become collective.

This idea led to the creation of a model of a cumulative effect, the basic assumption of which was that the relativistically invariant particle-production cross sections

$$\rho = \frac{1}{\sigma_{\text{in}}} E \frac{d^3\sigma}{d\mathbf{p}}$$

can be represented in the form

$$\rho = \Sigma_N p_N \rho_N,$$

where p_N is the probability of production of a group (droplet) of N constituents (nucleons, quarks, or partons), and ρ_N are the single-particle distributions that describe the particle production resulting from a collision of a particle with this group. With regard to ρ_N, it is assumed that it is a universal function that can be taken from particle-collision experiments. Such a model permitted the prediction[87] of the ratios of the cross sections for meson production in the reactions

$$p + A \to \pi^- + X \quad \text{and} \quad d + A \to \pi^- + X.$$

It was also predicted that there is a high probability for production of pions with energy 5–7 GeV in interactions of

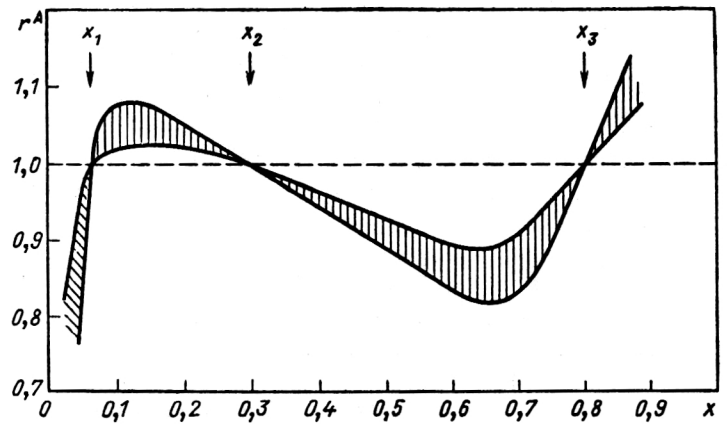

FIG. 22. Schematic representation of ratios of structure functions or cross sections for deep inelastic scattering of leptons by the nuclei A and D.

8-GeV deuterons with nuclei. An experiment made in 1971 completely confirmed this estimate.[88]

The success of this approach justified the introduction of the concept of a quark–gluon nuclear structure function. In the model of Ref. 90 proposed by Baldin, it is assumed that production of hadron a with a large value of the variable x_s (see below) in the reaction $\mathrm{I}+\mathrm{II}\to a+X$ in the limiting-fragmentation region can be described as the result of individual collisions of the quarks of the fragmenting hadron I with the quarks and gluons of the target nucleus II. The spectator quarks, which have avoided collisions, carry the fraction x_s of the momentum of nucleus II. On the "soft" hadronization of these quarks into mesons, it can be assumed that the distribution of the mesons with respect to x_s is the same as the distribution of the quarks in the nucleus.

In the region of applicability of the fragmentation model, the cross section for inclusive production of hadron a can be expressed in the form

$$E_a\frac{d^3\sigma}{d\mathbf{p}_a}=\text{const}\,A_{\mathrm{I}}^{1/3}G_{\mathrm{II}}(x_s,A),$$

where

$$G_{\mathrm{II}}(x_s,A)=\text{const}\,A_{\mathrm{II}}^{m(x_s)}\exp(-x_s/\langle x_s\rangle),$$

and the exponential determines the dependence of the quark–parton structure function G_{II} of nucleus II on the variable x_s, while the term $A_{\mathrm{II}}^{m(x_s)}$ describes its dependence on the atomic mass of the nucleus. The variable x_s is introduced in order to take into account the masses that participate in the reactions of the particles,[91] and in the limit of negligible masses it becomes the Bjorken variable x. It was found that for $0.6\leqslant x_s\leqslant 1.0$ the exponent of the A dependence satisfies the relation

$$m(x_s)=2/3+x_s/3,$$

while for comparatively heavy nuclei ($A>20$) at $x_s>1.0$ it is approximately equal to unity.

The kinematic region in which the proposed model can be used to study the quark–parton nuclear structure function in hadron–hadron collisions is determined by two criteria:[92]

1) $x_s>1.0$;

2) $b_{ik}=-(p_i/m_i-p_k/m_k)^2>5.0$,

where p and m are the 4-momenta and masses of the particles.

The parameter b_{ik} is the relative 4-dimensional velocity. For example, one can say that the condition $b_{ik}>5.0$ is satisfied by cumulative pions and kaons produced in proton–nucleus (or nucleus–nucleus) collisions at energy of the incident nucleus of about 3.5 GeV/nucleon and higher.

Even before the influence of the nuclear medium on the structure function of the free nucleon was detected in the experiments on muon deep inelastic scattering by iron and deuterium (the EMC experiment), investigations of the cumulative production of mesons in hadron–hadron reactions made it possible to study several effects indicating the impossibility of reducing the nuclear structure function introduced in this manner to the sum of the structure functions of the free nucleons. In particular, the following discoveries were made:

1) A universal x_s dependence of the inclusive cross sections for production of $\pi^{\pm}$ and $K^{\pm}$ mesons measured on many nuclei.[93,94] The structure functions $G_{\mathrm{II}}(x_s,A)$ calculated from these cross sections are shown in Fig. 23a in the kinematic region $0.6<x<3.0$. For comparison, we also give preliminary results of an estimate of $F_2^A(x)$ in muon deep inelastic scattering by carbon.[79] One can see the analogy in the behaviors of F_2^A and G_{II}, and also that in the hadron–hadron experiments there exists a possibility, in the framework of the considered model, of studying nuclear structure in a region of x that is as yet inaccessible in lepton experiments because of the small value of the cross sections.

2) A specific A dependence of the structure function G_{II} at a fixed value $x_s>1.0$. For example, the ratio of the cross sections for inclusive production of pions on nucleus A to the analogous cross section σ^{Pb} on lead increases logarithmically at small values of A, while for $A>30$ there is an indication of the apperance of a plateau.[95]

3) A characteristic minimum in the x_s dependence of the ratios of the cross sections for pion production on lead and on light nuclei (deuterium, helium, aluminum) in the region $x_s\approx 0.6$ (Ref. 93, Fig. 23c). Qualitatively, the picture agrees with the observations in experiments of lepton deep inelastic scattering by nuclei (Figs. 4 and 22). These results are particularly interesting in the region $x_s>1.0$, where nuclear effects must play a decisive role.

Production of J/ψ in leptonic and hadronic processes

If in particle interaction processes there is a significant contribution of gluons, as, for example, in production of the J/ψ particles, then the distortion of the quark distribution function under the influence of the nuclear medium will necessarily be reflected in the gluon distribution function. This happens because the gluon and quark momentum distributions are coupled through complementary processes of gluon and quark emission and the production of quark–antiquark pairs by gluons.

Nuclear effects of this type were studied by the EMC collaboration.[96] Measurements were made of the yields of J/ψ particles produced in muon deep inelastic scattering by nuclei of iron, deuterium, and hydrogen (the total numbers of events were 1212 ± 50, 225 ± 16, and 110 ± 11, respectively). To increase the statistics, the data obtained using hydrogen and deuterium were combined, and then the ratio of the single-nucleon cross sections for production of J/ψ on iron and on the averaged nucleon was calculated at muon energy 280 GeV:

$$r^{\mathrm{Fe}}=1.45\pm 0.12_{\mathrm{stat}}\pm 0.22_{\mathrm{syst}}. \qquad (34)$$

The large systematic errors in this result mean that one cannot with certainty say that in this experiment a larger cross section for production of J/ψ on nuclei than on nucleons was observed. Moreover, the result was not con-

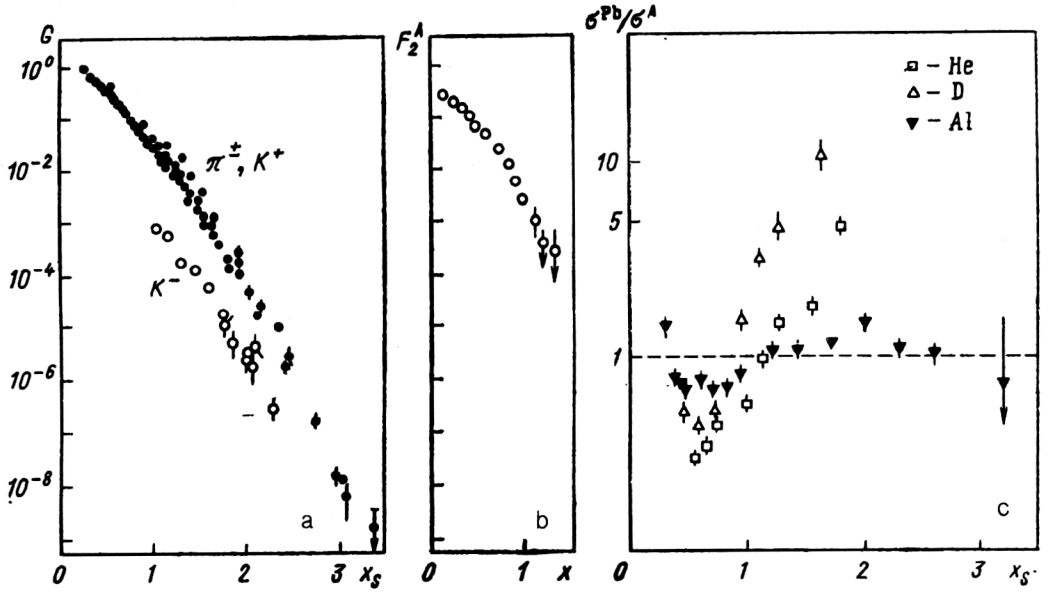

FIG. 23. Structure functions of nuclei G and F_2^A determined from inclusive cross sections for large-angle production of pions and kaons by protons (a, Ref. 93) and also in deep inelastic scattering of leptons by nuclei (b, Ref. 79) and ratios of cross sections for inclusive production of pions by protons on nuclei as functions of the parameter x_s (c, Ref. 92).

firmed by the data of other experiments on the photoproduction[97] and electroproduction[98] of the J/ψ particles.

An attempt was also made to determine the x dependence of the J/ψ yield and to relate it to the gluon distribution. It was shown that the cross section for virtual photoproduction of J/ψ has a Q^2 dependence that is well described by the expression $\sigma_\gamma(Q^2,\nu) = \sigma_\gamma(Q^2 = 0,\nu)/(1 + Q^2/M_\gamma^2)^2$, where $\sigma_\gamma(Q^2 = 0,\nu)$ is the J/ψ photoproduction cross section, and $M_\gamma = 2.9$ GeV. This relation was used for further estimates.

The photoproduction of J/ψ can be described in the framework of a model of photon–gluon fusion. In such an approach, the production of inelastic events is proportional to the density of hard gluons emitted by charmed quarks and, therefore, is proportional to the density of gluons in the target. It was shown[99] that such a model agrees well with the experimental data. It is assumed that the cross sections for elastic and quasielastic charmonium production can be explained by the emission of soft secondary gluons and, therefore, are also proportional to the density of gluons in the target. These considerations suggested to the EMC collaboration that the total inclusive cross section for J/ψ production should be proportional to the density of gluons per target nucleon. Following Ref. 100, it was assumed that the fraction of the nucleon momentum carried away by a gluon is $x \sim M_{J/\psi}^2/2M\nu$, where $M_{J/\psi}$ and M are the J/ψ and nucleon masses, respectively. With allowance for what was said above, we can write

$$\rho = [G(x,Q^2)_{\mathrm{Fe}}/G(x,Q^2)_{\mathrm{H,D}}]_{Q^2_{\mathrm{eff}}\sim M^2_{J/\psi}}$$
$$= \sigma_\gamma(Q^2 = 0,\nu)_{Fe/\sigma_\gamma}(Q^2 = 0,\nu)_{\mathrm{H,D}}$$
$$= (d\sigma/dE_{J/\psi})_{\mathrm{Fe}}/(d\sigma/dE_{J/\psi})_{\mathrm{H,D}}, \quad (35)$$

where $G(x,Q^2)$ is the density of gluons per nucleon at the effective 4-momentum $Q_{\mathrm{eff}} \sim M^2_{J/\psi}$. The gluon-density ratio calculated in this manner is shown in Fig. 24 as a function of the variable x. From our point of view, the large errors do not permit a definite conclusion to be drawn about the existence of an x dependence of this ratio in the range $0.026 < x < 0.085$, in which data were available. In other regions, such data do not exist.

Production of J/ψ on beryllium, copper, and tungsten nuclei was investigated at Fermilab[101] in beams of negative pions and antiprotons with momentum 125 GeV. The data were used to calculate the ratios R_1 of the W/Be and W/Cu cross sections as functions of the scaled variable x_F,

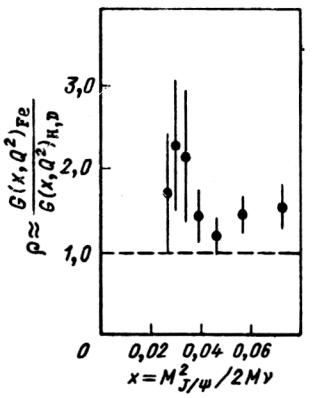

FIG. 24. Ratio of densities of gluons per nucleon measured in the EMC experiment[96] on iron, hydrogen, and deuterium.

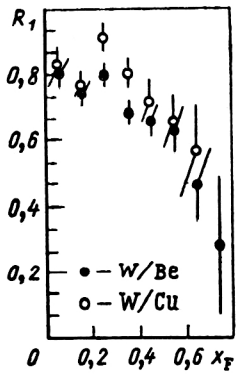

FIG. 25. Ratios of cross sections for J/ψ production on nuclei as functions of the scaled variable x_F.[101]

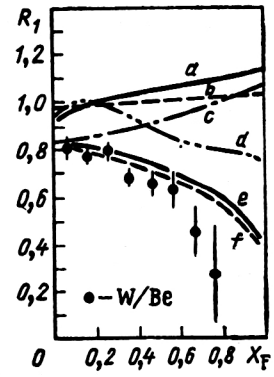

FIG. 26. Comparison of ratio of cross sections for J/ψ production on tungsten and beryllium nuclei[101] with theoretical calculations made under the assumptions that the nuclear medium distorts the distributions of the valence quarks in a nucleon [curves *a* (Refs. 127 and 128), *b* (Ref. 114), *c* (Refs. 137 and 142)] and that the gluon structure functions are subject to distortion [curves *d* (Ref. 105), *e* (Ref. 106), *f* (Ref. 104)].

where $x_F = p_L^*/p_{max}^*$ is the ratio of the longitudinal momentum of the $\mu^+\mu^-$ pair from J/ψ decay to the maximal c.m.s. momentum:

$$R_1 = \frac{(1/A_1)\,/(d\sigma/dx_F)_{A_1}}{(1/A_2)\,/(d\sigma/dx_F)_{A_2}}.$$

The results obtained in the pion beam clearly demonstrated that the J/ψ yield from the heavier target was less than from the light target ($R_1 < 1$), with, moreover, R_1 decreasing with increasing x_F (Fig. 25). Within the errors, the nature of the decrease of R_1 with increasing x_F was the same for both target combinations.

The data obtained in the antiproton beam have a lower statistical accuracy but still indicate a decrease of R_1 with increasing x_F. The same tendency can be found in data obtained before the discovery of the EMC effect.[102] Analysis of the distributions with respect to the transverse momentum permitted the conclusion that the observed decrease of the J/ψ production efficiency is enhanced in the region of small p_T.

The interpretation of these results in terms of an effect of the nuclear medium is not so obvious as in the cases when it is possible to compare data obtained on a heavy target and on hydrogen or deuterium. Nevertheless, the authors made calculations of the ratios of the cross sections measured in the pion beam on tungsten and beryllium targets in some models that took into account the distortion of the valence-quark distribution function in accordance with the EMC observation. The curves in the upper part of Fig. 26 show that the results of these calculations contradict the data. This was to be expected, since it is not the contribution of the valence quarks but that of the gluons that is dominant in J/ψ production.

In the simple gluon model proposed in Ref. 103, the J/ψ are produced in a process of fusion of two gluons:

$$G + G \to J/\psi + G. \tag{36}$$

However, the experimentally measured J/ψ production cross section is appreciably greater than what such a model predicts. The model also cannot explain the differences in the x dependences of the cross sections measured on light and heavy nuclei.

In Ref. 104, there was proposed a mechanism of three-gluon fusion:

$$A + B \to GGG \to J/\psi + X, \tag{37}$$

which requires one or two gluons of the beam particle A to fuse with two or one gluons of the target B. It is obvious that the importance of the process (37) increases for heavy nuclei, since with increasing atomic mass of the nucleus the probability of detecting an additional gluon in the target nucleus increases. Combination of two target gluons leads to a harder effective momentum distribution of the gluons, and this must be reflected in a decrease in the J/ψ production cross sections at large x. Another mechanism responsible for the discussed nuclear effect could be nuclear screening[105] in which there is an appreciable weakening of the soft gluon component of the nucleon through absorption of gluons by nucleons of the ambient nuclear medium.

The calculations showed that the nuclear screening mechanism gives a poor explanation of the experimentally observed decrease of R_1, whereas the model of three-gluon fusion (curve *f* in Fig. 26) satisfactorily follows the experimental dependence.

However, one can propose a further mechanism to explain the observed effect—the rescattering model of Ref. 106. What happens is scattering of the incident pion on a neighboring nucleon before the instant of J/ψ production or scattering of the produced J/ψ. It is obvious that in these cases J/ψ production on the heavy targets will be suppressed. The calculations made in the framework of this model are shown in Fig. 26 by curve *e*. As can be seen from comparison with the experimental data, this mechanism is in qualitative agreement with them.

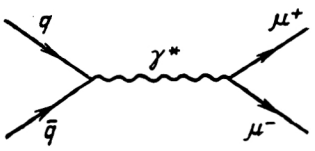

FIG. 27. Diagram of Drell–Yan process for production of lepton pairs.

Production of muon pairs

The production of muon pairs in collisions of hadrons is an alternative (to lepton deep inelastic scattering) method for investigating nuclear effects in the nucleon structure functions. In accordance with the mechanism proposed by Drell and Yan, the production of lepton pairs in the nonresonance region can be explained by a quark annihilation process with the diagram shown in Fig. 27.

An experiment to study this reaction was made at CERN[107] in a beam of negative pions with energies 140 and 286 GeV. The distributions of massive muon pairs produced on tungsten and deuterium targets were studied. Comparison of the measured cross sections with calculations in the framework of the quark–parton model make it possible to test the EMC effect in the timelike region of 4-momentum transfers. Events are selected in order to exclude the region of masses corresponding to production of particles of the J/ψ and Y families. The data were corrected for rescattering effects by means of Monte Carlo calculations. The corrections are negligibly small for the ratio of the cross sections as a function of the variable $x_2 = M^2/2p_2q$, where M is the mass of the dimuon pair, q is its 4-momentum, and p_2 is the 4-momentum of the target nucleon, this variable corresponding to the variable x measured in lepton deep inelastic scattering. Corrections were also introduced because the tungsten target was not isoscalar; these were small for the differential distributions, and in sum reached 7%. The authors showed that, as was expected from QCD, the pion structure function measured on the tungsten nucleus does not differ from the one measured on the deuteron. In contrast, the ratio of the cross sections for dimuon production on tungsten and on deuterium decreases with increasing value of the variable x_2, repeating the EMC effect for the structure functions F_2 (Fig. 28). For quantitative comparison of these two effects,

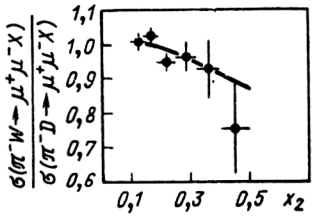

FIG. 28. Ratio of cross sections for production of massive lepton pairs on tungsten and deuterium nuclei.[107] The curve gives the results of calculations in accordance with a model in which the BCDMS results of Ref. 49 are used for the quantitative description of the effect of distortion of the distribution of the valence quarks in a nucleon.

calculations were made of the ratios of the cross sections for the production of dimuon pairs on the basis of the ratio $r^A(x)$ of the iron and deuteron structure functions measured by the BCDMS collaboration.[49] This was done by means of a model in which it was assumed that the quark distributions factorize, that their distortion by the nuclear medium is the same in tungsten and in iron, and that the nuclear medium has the same effect on the distributions of the valence and sea quarks. The ratio predicted in this way (with allowance for the acceptance and resolution of the experimental facility) is shown in Fig. 28 by the continuous curve. The good agreement with the experimental result demonstrates the presence of the same effect of the nuclear medium in the production of massive dimuons as is detected in the deep inelastic scattering of muons by nuclei.

6. MODELS OF THE EMC EFFECT. PREDICTIONS FOR EXPERIMENT

The experiments made to measure the structure functions $F_2^A(x,Q^2)$ and $F_2^D(x,Q^2)$ in lepton deep inelastic scattering that we have considered above demonstrated directly that the momentum distribution of the quarks measured in nuclei differs significantly from the distribution of the quarks in the free nucleon. By itself, this fact is a strong indication of the discovery in the nucleus of quark effects. Nevertheless, many authors insist that explanations of the EMC effect traditional for nuclear physics have not yet been completely exhausted; alternatively, they allow the possible existence of some exotic behavior in nuclei not associated with quarks. From our point of view, exposition of all the models proposed to explain the EMC effect advances us little in our understanding of the essence of the phenomenon. For this reason, we restrict ourselves to a survey of the basic approaches that differ in fundamentals.

The role of nuclear structure effects

In the standard approach for nuclear physics, the nuclear structure function $F_2^A(x,Q^2)$ is determined by means of the expression (17). Before the discovery of the EMC effect, it was assumed that the function $f_N(z)$ in (18) is determined by the nucleon momentum distribution $\rho(\mathbf{p})$, normalized to unity:

$$\int d^3\mathbf{p}\rho(\mathbf{p}) = 1,$$

$$f_N(z) = \int d^3\mathbf{p}\rho(\mathbf{p})\delta(z - pq/M_N\nu) \approx \int d^3\mathbf{p}\rho(\mathbf{p})\delta[z - (\mathbf{np} + M_N)/M_N], \quad (38)$$

where $\mathbf{n}$ is the unit vector along the momentum transfer: $\mathbf{n} = -\mathbf{q}/|\mathbf{q}|$.

To explain the EMC effect, the authors of Ref. 108 proposed that the expression (38) should be modified as follows:

$$f_N(z) = \int d^3\mathbf{p}\rho(\mathbf{p})\delta[z - (\mathbf{np} + M_A - M)/M_N], \quad (39)$$

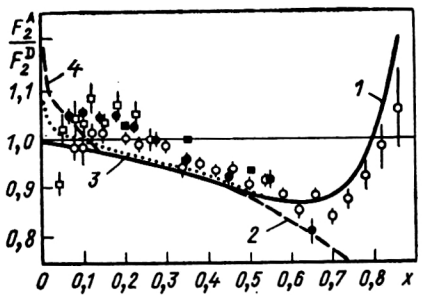

FIG. 29. Description of nuclear effects in the nucleon structure function: *1*) based on allowance for Fermi motion in the approach proposed in Ref. 108; *2*) corresponding to calculation without allowance for Fermi motion; *3*) and *4*) contribution of meson exchange currents calculated for two values of the parameter that determines the pion density. Experiments: black circles, Ref. 49; black squares, Ref. 46; open circles, Ref. 39; open squares, Ref. 50.

where M is the mass of a heavy inert particle introduced to represent the nuclear medium surrounding the nucleon. This particle and the active nucleon bound to it form a nucleus with mass M_A. It is assumed that the active nucleon moves in the target with nonrelativistic velocity. Then the energy ε of separation of the nucleon from the nucleus is

$$\varepsilon \equiv M_N + M - M_A. \tag{40}$$

The mean longitudinal momentum of the nucleon is given by

$$\langle z \rangle = A^{-1} \int dz z f_N(z) = 1 + \langle \varepsilon \rangle / M_N < 1. \tag{41}$$

The sum rule obtained in Ref. 108 for the ground state of the nucleus made it possible to determine the parameter mean values $\langle \varepsilon \rangle$ and $\langle z \rangle$ for the iron nucleus:

$$\langle \varepsilon \rangle_{\mathrm{Fe}} = -39 \text{ MeV}, \quad \langle z \rangle_{\mathrm{Fe}} = 0.96.$$

The ratio of the structure functions calculated in this approach decreases with increasing variable x in approximately the same way as the experimentally measured ratio if $x < 0.6$. This result is shown in Fig. 29 by the broken curve. To explain the experimentally observed growth of $r^A(x)$ when $x < 0.7$, it is sufficient to use in the calculations the simplest nuclear model—the model of a Fermi gas of nucleons in a potential well V. The result obtained by the authors for $V = -62$ MeV agrees satisfactorily with the result of the SLAC experiment[39] and is shown in Fig. 29 by the continuous curve.

As can be seen from the expression (41), in this model the sum rule for the momenta of the nucleons in the nucleus is violated. There is a simple way of satisfying the energy conservation law. For this, it is sufficient to consider the additional contribution to the energy ground state of the nucleus from the meson fields. Most probably, this must be the contribution from the pions, so that the range of the variable x in which it will be appreciable is situated at $x < m_\pi/M_N$. Allowance for this contribution leads to an increase of $r^A(x)$ in the region of small values of x, whereas the experimental data demonstrate that $r^A(x) < 1.0$. This is not the only shortcoming of the model. A fundamentally important discrepancy between the model and the experimental data is observed in the range $0.3 < x < 0.35$. As was demonstrated in Sec. 4, the data indicate that in this region $r^A(x) = 1$, but the result of the model lies significantly lower.

There are also objections to the method used in Ref. 108 to calculate the parameters $\langle \varepsilon \rangle$ and $\langle z \rangle$ and to the normalization of the nuclear vertex function.[109,110] Using the Hartree–Fock approach with allowance for density-dependent interactions, the authors of Ref. 109 found that

$$\langle \varepsilon \rangle = -26 \text{ MeV}, \quad \langle z \rangle = 0.972.$$

Such a change of the parameters significantly reduces the dip in the ratio $r^A(x)$ at $x \sim 0.6$ and makes the agreement with the experimental data still worse. Thus, we conclude that the model for describing the nuclear effects by taking into account the binding energy of the nucleons and their Fermi motion in the nucleus does not provide a quantitative explanation of the observed effect.

The agreement between the theory and experiment is significantly improved by a relativistic treatment of the lepton–nucleus interaction. In Ref. 111, it was suggested that r^A should be calculated by means of a relativistic model that had worked well in explaining several aspects of nuclear interactions at high energies.[112] In this model, it is assumed that nucleons are the only constituents of a nucleus. The normalization of the distribution function $G_{a/A}(\mathbf{Y}, \mathbf{k}_T)$, which is the probability of finding in nucleus A the consistuent a with partial momentum $\mathbf{Y}$ and transverse momentum $\mathbf{k}_T$, is chosen in such a way that the sum of all the partial momenta is equal to the total momentum of the nucleus. In this approach, the total number of particles, which can be obtained by integrating $G_{a/A}$ and summing over all degrees of freedom, is not fixed. As in the parton model, the production of particle pairs is allowed here. In contrast to the model of Ref. 108, this approach permits a correct description of the behavior of the ratio r^A in the region $x \sim 0.3$. Independently of the atomic mass of the nucleus, the ratio is $r^A = 1.01$ at $x = 0.333$, in good agreement with the experimental results. However, in this model the region of small values of x is not described well.

The need for a relativistic treatment of nuclear structure was also deduced by Efremov,[113] who saw shortcomings of many models of the EMC effect in the way they represent the nucleus as a bound state of A nucleons. In the framework of a relativistic approach, an interacting system such as a nucleus must be regarded as a system with a variable number of particles. Only the baryon number, i.e., the number of nucleons minus the number of antinulceons, is conserved. The calculations made in this model agree well with the measurements of $r^A(x)$ by the BCDMS[47,49] and SLAC[39] groups. An interesting consequence is that in the model the relation $r^A(x) = 1.0$ must hold independently of A at $x \approx 0.25$.

Thus, in the framework of ordinary nuclear models it is possible to achieve a qualitative description of the EMC effect in the region $0.3 < x < 0.8$. However, the parameters

needed for this give rise to objections. In addition, this approach cannot pretend to explain the effects in the region $x<0.3$.

Change of scale of the 4-momentum transfer

As is well known, the nucleon structure function is a function of the variables x and Q^2, and it decreases monotonically with increasing Q^2, namely, $F_2(x,Q_2^2)/F_2(x,Q_1^1) < 1$ if $Q_2^2 > Q_1^2$, which resembles the EMC effect. This suggests that the structure functions of the nucleus and of the nucleon used to calculate the ratio $r^A(x)$ are measured at different effective values of Q^2, i.e., in the experiments on nuclei the scale of measurement of the variable Q^2 is changed.

The evolution of the nucleon structure function $F_2(x,Q^2)$ with Q^2 is explained in QCD by a gluon-emission process:

$$q \to q + g. \tag{42}$$

According to the model of Ref. 22, the distribution function of the valence quarks is determined by its value in the region $x \leqslant y \leqslant 1$ and by the probability $P_{qq}(x/y)$ of the transition $q(y) \to q(x)$:

$$\frac{dq_v(x,t)}{dt} = \frac{\alpha_s(Q^2)}{\pi} \int_x^1 \frac{dy}{y} q_v(y,t) P_{qq}\left(\frac{x}{y}\right), \tag{43}$$

where

$$t = \ln(Q^2/\mu^2). \tag{44}$$

The scale parameter μ^2 in (44) is a cutoff parameter, which makes it possible to avoid a divergence in the integral over the transverse momentum of the gluon radiated in the process (42).

The main assumption made by the authors of Refs. 114–118 is that the change of the distribution function q_v of a nucleon bound in a nucleus from that of the free nucleon is determined by the parameter μ^2, which is not related to the QCD scale parameter Λ. The features observed in the EMC effect require $\mu_A^2 < \mu_N^2$. Then a softer (with respect to the variable x) distribution of the quarks in a nucleus can be explained by the emission of gluons, which transform $Q_2^2 = \mu_N^2$ into $Q_1^2 = \mu_A^2$. At the same time, it is assumed that

$$q^N(x,Q_2^2 = \mu_N^2) = q^A(x,Q_1^2 = \mu_A^2).$$

Actual calculations in such a model require nuclear-structure data. In Ref. 116, the ratio μ_N^2/μ_A^2 is related to the ratio λ_A/λ_N of parameters that determine the nucleon sizes:

$$\lambda_A/\lambda_N = 1 + (2^{1/3} - 1)V_A, \tag{45}$$

where V_A is the probability of overlapping of spheres whose radii is determined by the nucleon charge radius. For $V_A \neq 0$, $\lambda_A > \lambda_N$, and, therefore, the physical size of the nucleon in the nucleus is greater than that of the free nucleon. The observed EMC effect requires $\lambda_A/\lambda_N \approx 1.15$. In other words, in the iron nucleus one should observe a "swelling" of the nucleon by 15%.

The relationship between the structure functions proposed in this model has the form

$$F_2^A(x,Q^2) = F_2^N[x,\xi(Q^2)Q^2], \tag{46}$$

where

$$\xi(Q^2) = \xi(Q_0^2)^{\alpha_s(Q_0^2)/\alpha_s(Q^2)}, \tag{47}$$

in which α_s is the QCD running constant. At $Q^2 = 20$ GeV^2, $\xi = 2.02$ for the iron nucleus.

The calculations that were made showed that the model does not agree well with the experimental data in the region of small values of x. To construct the model, it was assumed that the scaling hypothesis is valid at $x \approx 0.1$. For this reason, the model predicts $r^A(x_1) = 1$ at $x_1 = 0.1$, whereas experiment gives $x_1 \approx 0.33$. In addition, the model cannot be used in the range $x > 0.7$, where correct allowance for the two-nucleon interaction dynamics is important.

The authors of several other studies also attempt to explain the EMC effect by an increase in the radius of a nucleon bound in a nucleus (see, for example, Refs. 119–121). The same idea results from the hypothesis of color conductivity,[76,122] or Q^2-dependent color confinement for partons within a nucleus. At the same time, the cutoff parameter μ_A^2 in the expression (44) is related to the nuclear radius, the parameter ξ (47) is related to the ratio of the squares of the radii of the nucleus and nucleon, and the expression (46) takes the form

$$F_2^A(x,Q^2) = F_2^N(x,Q^2R_A^2/R_N^2). \tag{46'}$$

Quantitatively, it does not correspond well to the experimental data. A distinctive feature of this model is the circumstance that for each species of nucleus it is necessary to introduce a corresponding QCD scale parameter Λ, and this is not confirmed by experiment.[69]

The "swelling" of nucleons in a nucleus, if it exists, must be due to internal properties of the nucleon independent of the kinematics of the interaction process. For this reason, it is sufficient in testing the possible increase of the nucleon radius to analyze the results of experiments on electron scattering by nuclei in the region of small 4-momentum transfers. In this respect, the most interesting experiment was the one of Ref. 123, made at SLAC in order to study quasielastic electron scattering by ^{3}He nuclei. The largest value of Q^2 achieved in this experiment was 4 GeV^2. The authors showed that with high accuracy the inclusive cross section for electron scattering is a function of the single variable $y = \mathbf{k}\cdot\mathbf{q}/q$, where $\mathbf{k}$ is the momentum of the nucleon in the nucleus, and $\mathbf{q}$ is the momentum transfer to the nucleon by the electron:

$$\frac{d\sigma(Q^2,\omega)}{Z\sigma_p + N\sigma_n}\, d\omega = F(y)dy.$$

This phenomenon was called y scaling. Its interpretation is based on the single-particle nature of the quasielastic scattering process. If one attempts to change the scale of the Q^2 dependence of the nucleon form factors, which determine the values of the cross sections σ_p and σ_n, this imme-

diately leads to violation of the y scaling. This circumstance makes it possible to establish a limit on the possible changes of the nucleon radius R^A in a nucleus from the radius r_N of the free nucleon, namely,

$$R^A \leqslant 1.03 r_N. \tag{48}$$

Analyzing the results of the experiment of Ref. 38 on electron deep inelastic scattering by aluminum and deuterium nuclei, the authors of Ref. 124 obtained a similar restriction on the possible increase in the radius of a nucleon bound in a nucleus. These restrictions demonstrate that the picture of the distortion of the nucleon structure function constructed in models of a change in the scale of the variable Q^2 (Refs. 114–118) and the color dielectric model[76,122] do not reflect the nature of the EMC effect.

In Ref. 125, an attempt was made to obtain the basic properties of nuclear matter by means of QCD sum rules, with allowance for quark and gluon confinement. One of the results was a predicted increase of the size of a nucleon in nuclear matter by about 3%, in good agreement with the estimate (48).

However, there also exist other QCD approaches to the problem of the change in the properties of nucleons in a nucleus. A confinement model was constructed with allowance for interpretation of the QCD vacuum as a superconductor for the chromomagnetic field,[126] and a consequence of it is a possible increase in the radius of a nucleon in a nucleus by up to 40%, a result that, as we see, is not confirmed experimentally.

These examples demonstrate the possibility of using distortion of the nucleon structure in a nuclear medium for a critical test of models that describe the confinement mechanism.

Effects of pions in nuclear structure

It was noted earlier that to improve the agreement between the experimental data and calculations made with allowance for the binding energy of nucleons in a nucleus the pion model of Ref. 108 can be used. The pion-exchange model was one of the first models used to explain the EMC effect,[127–130] since the widely adopted approach for constructing nuclear forces, describing the interaction of two nucleons at intermediate and large distances, consists of consideration of the $NN\pi$ vertex. A natural consequence of such an interaction for a nuclear medium is the presence in a nucleus of constituent exchanged pions. The diagram that describes this vertex is given in Fig. 30, in which z denotes the fraction of the nucleon momentum carried away by the pion. It is the loss by the nucleon of the momentum fraction $\langle z_N \rangle = 1.0 - z$ that leads to the observed decrease of $r^A(x)$ with increasing x. According to the calculations of Ref. 129, the momentum fraction z varies weakly with the atomic mass of the nucleus. For example, for the Al nucleus $z = 0.049$, for the Fe nucleus it is 0.052, and for the Au nucleus it is 0.061. This parameter is responsible for the behavior of the ratio r^A in the region of central values of x, where $r^A < 1.0$.

A second important parameter of the model is the mean number of pions $\langle n_\pi \rangle$ per nucleon of the nucleus.

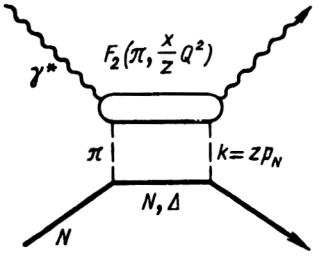

FIG. 30. Diagram describing the contribution of one-pion exchange to the nucleon structure function.

The dependence of this parameter on the atomic mass A is calculated by a method analogous to the expression (46),[129] and there is little variation from nucleus to nucleus:

Type of nucleus:	Al	Fe	Au
$\langle n_\pi \rangle$:	0.089	0.095	0.114

It should be borne in mind that the accuracy estimated by the authors for the calculation of $\langle n_\pi \rangle$ is $\pm 30\%$. The role of this parameter is to be responsible for the excess of the ratio $r^A(x)$ above unity in the region of small x. If it is recalled that in the very first publication of the discovery of the EMC effect[10] the excess of $r^A(x)$ in the region $x < 0.2$ reached 17%, it becomes clear that the pion models are most suitable for describing the effect. The comparison of the calculation of $r^A(x)$ in the pion model with modern data on the EMC effect is shown in Fig. 31 by the continuous curve. The broken curve shows the results of calculations in the model with change of the scale of Q^2 (Ref. 114). One can speak of qualitative agreement of the pion model and the experimental data in the region $0.2 < x < 0.6$. To explain the region of smaller values of x, one must also consider the screening effect. The region $x > 0.6$ is also difficult for the model, since it is necessary to use approximate calculations of the high-momentum nucleon component in the nucleus.

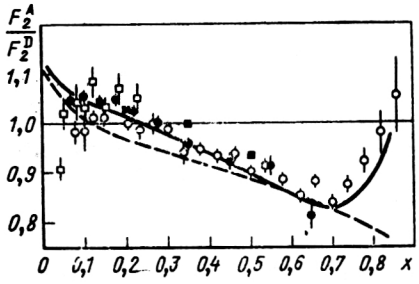

FIG. 31. Comparison of results of experimental investigation of nuclear effects in the nucleon structure function with theoretical calculations made in the pion-exchange model (continuous curve)[127] and the model with a change in the scale of Q^2 (broken curve, Ref. 114): open circles, Ref. 49; black squares, Ref. 46; open circles, Ref. 39; open squares, Ref. 50.

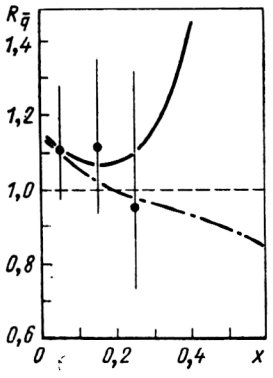

FIG. 32. Ratio of distribution functions of sea quarks in the iron nucleus and proton measured in deep inelastic scattering of antineutrinos.[57] The continuous curve shows the predictions of the pion exchange model,[129] and the chain curve is for the change-of-scale model.[114]

At the same time, this model gives interesting predictions for neutrino experiments. For example, Fig. 32 gives the results of calculation of the ratio $R_{\bar{q}}(x)$ of the distribution functions of the sea quarks in the iron nucleus and in the free nucleon obtained in the pion model (continuous curve) and in the model with change in the scale of Q^2. The increase in the fraction of antiquarks in the nucleus in the pion model occurs because of exchange of pions containing valence antiquarks. For comparison, Fig. 32 gives the results of the neutrino experiment of Ref. 57, in which the ratios of the antiquark distribution functions were measured:

$$R_{\bar{q}}(x) = \frac{(1/2)(\bar{d}+\bar{u}+2s)_{\mathrm{Fe}}}{(\bar{d}+s)_{\mathrm{H}}}. \qquad (49)$$

It is obvious that under the reasonable assumption $\bar{u}=\bar{d}$ the expression (49) corresponds to the ratio of the contributions of the sea quarks in the nucleus and in the free nucleon. To test these models, accurate experiments on neutrino deep inelastic scattering by nuclei are needed.

Multiquark states in nuclei

Even before the discovery of the EMC effect, quark models were used not only to describe the structure and spectroscopy of hadrons but also to describe short-range nuclear forces. The quantitative predictions of many models differed strongly if they were based on different mechanisms of quark confinement. Reviews of theoretical studies devoted to possible manifestations of quark–gluon degrees of freedom in nuclei can be found in Refs. 11, 131, and 132.

The need for development of the quark–parton model of nuclear structure was first mentioned in the studies of Refs. 88–90, which were associated with investigation of inclusive production of mesons in hadron collisions. According to the results of Ref. 89, obtained in 1974, the traditional approach using a model of Fermi motion to explain the deformation of the wave function of a nucleon bound in a nucleus is inadequate in the region $x>0.6$. As the EMC experiment showed,[10] the region in which this approach becomes invalid begins even earlier, at $x\sim 0.3$.

We shall consider some studies in which quark models were used to describe deep inelastic scattering of leptons by nuclei. Most of them were devoted to calculations of the structure functions and of the ratio $r^A(x)$ in the region $x<1.0$, where the results of high-precision experiments were available.

In Ref. 133, the structure functions $F_2^A(x,Q^2)$ measured on ^{3}He nuclei[134] in the range $1 < Q^2 < 4$ GeV^2 were successfully described. This was done on the basis of a phenomenological approach allowing the formation, with a certain probability, in a nucleus, of three-, six-, and nine-quark clusters. The momentum distribution of the quarks in a cluster was obtained on the basis of the quark counting rules.[135,136] Good agreement with experiment was achieved. It was found that the probabilities of formation of three-, six-, and nine-quark clusters are 0.83, 0.16, and 0.01, respectively.

It is therefore natural that immediately after the discovery of the EMC effect was published a proposal was made to explain it by partial deconfinement of the quarks in the iron nucleus.[137] Such a proposal is sufficient to obtain a distribution function of the valence quarks that decreases with increasing x more strongly in a nucleus than in a nucleon. The results of this study were only qualitative. Quantitative calculations of the EMC effect on different nuclei were made in Ref. 138, in which it was assumed that six-quark objects could form in a nucleus. Making the assumption that the radius of such an object was related to the nucleon radius by

$$R_{6q} = 2^{1/3} R_{3q},$$

the authors predicted that $r^A(x)$ for $Q^2 = 20$ GeV^2 and $x=0.55$ would be reduced by 10% at $A=50$. This result agrees well with the experiment made at SLAC[39] (see Fig. 15b). However, the prediction of a weakening of the A dependence of the variation of r^A for sufficiently heavy nuclei was not confirmed.

The attempts of theoreticians to find the best description of the EMC effect led to the appearance of numerous studies[139–151] using the idea of the existence, in a nucleus, of multiquark configurations. The nuclear structure function $F_2^A(x)$ calculated in the framework of such an approach can be expressed in the general case in the form

$$F_2^A(x) = \sum_c \int_x^A p_c(z) F_2^c(x/z)\,dz, \qquad (50)$$

where the summation is over the cluster type: $c=1, 2, 3,...$, corresponding to configurations of three, six, nine, etc., quarks. The structure functions F_2^c in the expression (50) are the structure functions of the quark clusters, and the case $c=1$ corresponds to the structure function of the free nucleon. The probability of finding a cluster of type c in a nucleus is denoted by p_c.

A problem common to all the models is the calculation of the structure functions F_2^c, for which the quark counting rules are used. Strictly speaking, the probabilities p_c for $c\neq 1$ can be determined only from the results of direct

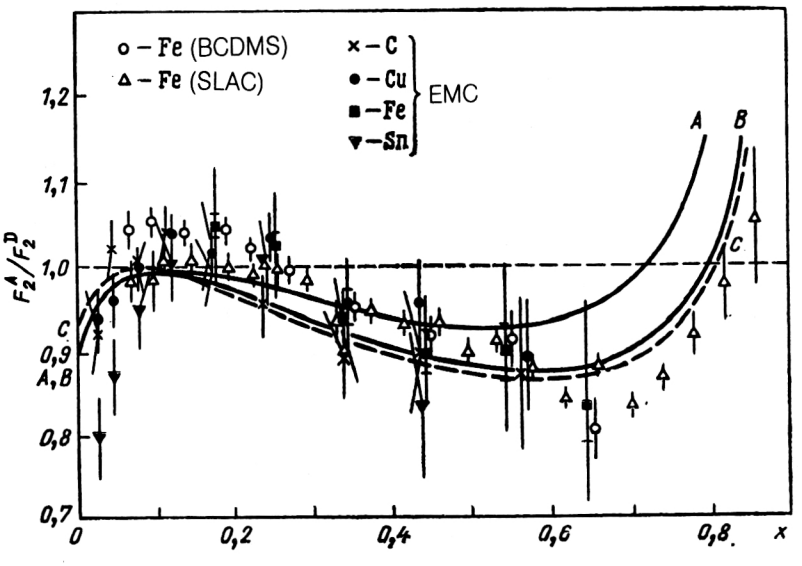

FIG. 33. Description of nuclear effects in the nucleon structure function by means of the quark-cluster model. The three curves correspond to different parametrizations of the six-quark cluster function: A) $a = 11$, $b = 9$; B) $a = 11$, $b = 10$; C) $a = 13$, $b = 10$.[147]

measurements of the structure functions of nuclei in the region $x > 1.0$. As long as such data are unavailable, p_c are determined from the condition of best agreement with the results of measurement of $r^A(x)$ at $x < 1.0$. Thus, the relative freedom in the choice of the model parameters ensures good description of the experimental data by practically all forms of the model.[139–151] The probabilities of six-quark clusters determined in this way are about 16% for the iron nucleus[141] (in Ref. 142, up to 30%). In Ref. 144, a dependence $p_c \sim A^{1/3}$ was proposed; for the beryllium nucleus this gives about 10%, for iron about 20%, and for gold about 30%.

Another characteristic feature of the multiquark models is the common problem that they have in describing r^A at $x < 0.2$. It was shown in Ref. 147 that this difficulty can be overcome by increasing the accuracy with which the quark distribution functions are parametrized. For example, to describe the distributions of the valence, V_N, and sea, O_N, quarks the authors chose the expressions

$$V_N(z) = B_N z^{1/2}(1-z)^{b_N}, \qquad (51)$$

$$O_N(z) = A_N(1-z)^{a_N},$$

where N denotes the number of quarks in the cluster. To determine the parameters a_N and b_N, the results of measurements of the structure functions of the pion and nucleon, regarded as the simplest clusters with $N = 2$ and $N = 3$, were used. The values obtained for b_N agree well with the dependence

$$b_N = 2N - 3, \qquad (52)$$

which was proposed on the basis of the quark counting rules (Refs. 135 and 136): $b_3 = 3, b_6 = 9$. The exponent for the distribution of the sea quarks is determined with much greater errors and is $a_3 = 9$, $a_6 = 11$. As the calculations showed, the uncertainty in this parameter has little effect on the results of the calculation of r^A, which are given in Fig. 33.

Intuitively, one would expect the probability of formation, in a nucleus, of a cluster of N quarks to decrease with increasing N. However, there exist approaches in which clusters with a larger number of quarks make a larger contribution to the nuclear structure functions. For example, in Refs. 148 and 149 the presence of α particles in a nucleus is required. Good agreement with experiment is achieved if the nucleus contains an admixture of such clusters of between 15 to 25%. In Ref. 150, 12-quark clusters in a nucleus not identical to α particles were considered. The authors obtained good agreement with the experimental data for $p_2 = 0.02$–0.06 and $p_4 = 0.15$ (0.2) for the aluminum (respectively, iron) nucleus. It is obvious that the studies of Refs. 148–150 cannot predict a smooth dependence of the EMC effect on the atomic mass of the nucleus. The maximal effect is expected for nuclei with a clearly expressed α-cluster structure: ^{4}He, ^{12}C, ^{16}O, etc. Judging from the results given in Fig. 15, such a dependence is not observed experimentally.

The study of Ref. 152 considered an increase of the effective confinement radius of clusters in the form

$$R_i = R_1 i^{1/3},$$

where i is the number of nucleons in a cluster. This approach gave a very accurate description of the A dependence of the measured ratio r^A. The authors also calculated the ratios of the distribution functions of the gluons in nuclei and in free nucleons, which are to be regarded as a prediction for an experiment.

To improve the agreement between the calculations and experiment, some authors also introduced into the quark models of the nuclear structure functions contributions of traditional mechanisms—meson exchange currents[143] or Fermi motion of the nucleons.[83,153] The meson fields make a contribution at small $x < m_\pi/M$, while a contribution of multiquark configurations is to be expected near the single-nucleon kinematic limit $x = 1.0$ and beyond it. Fitting of the results of the calculations to the available experimental data makes it possible to determine the probability of occurrence of the various conjectured mechanisms of distortion of the nucleon structure function

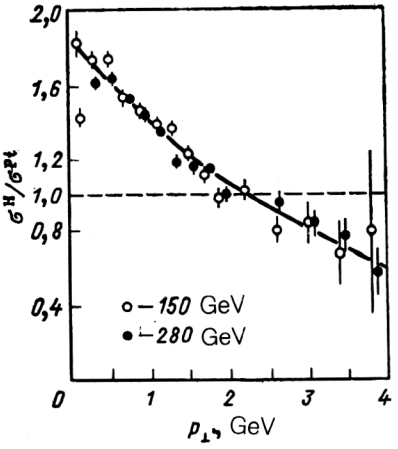

FIG. 34. Results of description of the ratio of cross sections for J/ψ production on hydrogen and platinum obtained in the framework of the additive quark model.[154]

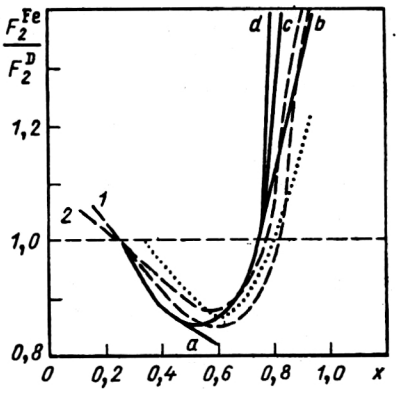

FIG. 35. Predictions of behavior of the ratio of structure functions obtained in the quark-cluster model (continuous curves), the flucton model (broken curves), and the model of few-nucleon correlations (dotted curve). The sensitivity of the models to the free parameters is shown by several versions of calculations: *1*) and *2*) calculations in which the ratio of the critical nuclear density to the normal density is 3.9 and 4.2, respectively; a) calculations in which the structure function of a multiquark cluster (up to $12q$ inclusive) decreases more rapidly than the structure function of a $6q$ cluster, c) at the same rate as the structure function of a $6q$ cluster, and d) slower than the structure function of a $6q$ cluster; b) obtained under the assumption that the radii of the multiquark bags are connected by $R_{12q} = 2^{1/3}R_{6q}$ (Ref. 137).

by the nuclear medium. For example, several hypotheses for the combination of two nucleons into a six-quark cluster were tested in Ref. 83. An analogy with the change of the collision time of two nucleons in a nucleus was used; depending on it, either the nucleons would not overlap at all, or one may find 2, 4, or 6 common quarks in the overlap region. The best agreement with the experimental data on $r^A(x)$ was achieved in the case of partial overlapping of nucleons having two common quarks.

Quark models successfully describe nuclear effects in processes of Drell–Yan type and the production of J/ψ particles[154] (see, for example, Fig. 34, which gives the ratio of the cross sections for J/ψ production by negative pions on protons and on platinum nuclei). An important part here is played by the correct description of the rescattering of the quarks in a nucleus, which leads to a change in the transverse momentum of a quark. The need for correct allowance for the rescattering mechanism was also pointed out by the authors of Ref. 155. They considered the semiinclusive deep inelastic scattering of neutrinos by nuclei[61] in which interactions with strongly and weakly bound nucleons of a nucleus are distinguished.

The main thing in the description of nuclear effects by means of the quark approach is that clusters with the number of quarks $N > 3$ can be formed. It is therefore obvious that the decisive test of such models will be made in the region of x values near $x = 1.0$ and for $x < 1.0$. Figure 35 gives the results of calculations of the expected behavior of $r^A(x)$ near $x = 1.0$ in Refs. 139, 143, and 150. A very characteristic dependence of this ratio on x is also expected in the framework of the model of Ref. 141 at $x > 1$. However, the capabilities of the currently existing experimental facilities do not permit testing of these predictions.

CONCLUSIONS

Observation of the effects of the change in the quark structure of nucleons under the influence of the nuclear medium surrounding them has demonstrated once more how an increase in the accuracy of an experiment can radically change established ideas about nuclear properties.

The experiments made using electron, muon, and neutrino beams to investigate the structure of nucleons bound in a nucleus have made it possible to determine the dependence of the nuclear effects on the Bjorken variable x and on the atomic mass of the nucleus A, and also to show that within the errors the nuclear effects do not depend on the 4-momentum transfer.

The theoretical models developed to describe the ratio $r^A(x) = F_2^A/F_2^D$ of the structure functions agree in the main details with the observed variation of r^A with variation of the Bjorken variable x in the range $0.07 < x < 0.8$. However the agreement between the calculations and the experimental data is not yet good enough to speak of a quantitative description of the phenomenon.

The great importance of a correct understanding of the nature of the observed phenomenon is indicated by the publication of more than 150 theoretical studies on it. This list will obviously be extended by new studies because the experimental investigations have presented the theoreticians with values of r^A with errors $\sim 1\%$. The approach based on quark models is the most promising. However, its possibilities are restricted by the insufficiently accurate parametrization of the quark distribution functions; in particular, the region $x > 0.8$ has been poorly studied.

We expect important new information about the nature of the nuclear effects in the structure functions to come from high-precision experiments on deep inelastic scattering of neutrinos and antineutrinos ($x < 1.0$), and also electrons and muons ($x > 1.0$) by nuclei. Such experiments would permit a critical tests of the models at $x \approx 0.3$ and $x > 0.8$, where the theoretical calculations of $r^A(x)$ differ most strongly, and, therefore, would permit the

choice, from the many possible mechanisms, of the one that is responsible for the observed effects.

We thank A. M. Baldin, whose comments enabled us to eliminate some shortcomings of the present review, and also A. V. Efremov and P. S. Isaev for helpful discussions of the problems of theoretical description of deep inelastic scattering of leptons by nuclei.

[1)]It is interesting to note that already before the publication of experimental results on measurement of the nucleon form factors Markov[19] discussed the possibility of constructing a relativistically invariant and unitary theory containing a "dynamically deformable form factor."

[2)]Strictly speaking, the processes (5) and (6) can also take place by means of exchange of the neutral intermediate boson Z^0, but the contribution of the corresponding diagram is small and in practice is taken into account only as a correction. Proofs of the existence of exchange of the Z^0 boson already before its direct detection were obtained in experiments on the scattering of electrons by deuterons at SLAC[20] and of muons by carbon nuclei at CERN.[21]

[3)]To ensure accurate correspondence between the observed cross sections and the theoretical ones expressed in terms of the nucleon structure functions, it is necessary to take into account the contribution to these cross sections of the radiative processes. They are taken into account most fully in the approach developed in Ref. 25.

[4)]The idea of volume fluctuations of nuclear matter was proposed by Blokhintsev[85] in 1957 in order to explain the knockout of high-energy deuterons from nuclei observed in Ref. 86.

[1]Particle Data Group, Phys. Lett. **204B**, 1 (1988).
[2]R. P. Feynman, *Photon–Hadron Interactions* (Benjamin, Reading, Mass., 1972) [Russ. transl., Mir, Moscow, 1975].
[3]M. Gourdin, Phys. Rep. **11**, 29 (1974).
[4]A. Buras, Rev. Mod. Phys. **52**, 199 (1980).
[5]M. Gell-Mann, Phys. Lett. **8**, 214 (1964).
[6]G. Zweig, CERN Preprint TH 401, Geneva (1964).
[7]J. D. Bjorken, *Enrico Fermi Summer School XLI, Varenna* (Academic Press, New York, 1967); Phys. Rev. **179**, 1547 (1969).
[8]M. Breidenbach, J. I. Fridman, H. W. Kendall *et al.*, Phys. Rev. Lett. **23**, 935 (1969).
[9]B. A. Arbuzov and A. A. Logunov, Usp. Fiz. Nauk **123**, 505 (1977) [Sov. Phys. Usp. **20**, 956 (1977)].
[10]J. J. Aubert, G. Bassompierre, K. H. Becks *et al.*, EMC Collaboration, Phys. Lett. **123B**, 275 (1983).
[11]A. M. Baldin, Fiz. Elem. Chastits At. Yadra **8**, 429 (1977) [Sov. J. Part. Nucl. **8**, 175 (1977)].
[12]N. N. Bogolyubov, Vestn. Akad. Nauk SSSR No. 6, 54 (1985).
[13]R. W. McAllister and R. Hofstadter, Phys. Rev. **98**, 217 (1955); Phys. Rev. **102**, 851 (1956).
[14]W. K. H. Panofsky and E. Alton, Phys. Rev. **110**, 1155 (1958).
[15]A. Baldin, Nucl. Phys. **18**, 310 (1960).
[16]V. I. Gol'danskiĭ, O. A. Karpukhin, A. V. Kutsenko *et al.*, Zh. Eksp. Teor. Fiz. **38**, 1665 (1960) [Sov. Phys. JETP **11**, 1201 (1960)].
[17]P. S. Baranov, G. M. Buĭnov, V. G. Godin, and V. V. Pavlovskaya, Pis'ma Zh. Eksp. Teor. Fiz. **19**, 777 (1974) [JETP Lett. **19**, 398 (1974)].
[18]L. D. Landau and E. M. Lifshitz, *The Classical Theory of Fields*, 4th English ed. (Pergamon Press, Oxford, 1975) [Russ. original, Nauka, Moscow, 1988].
[19]M. Markov, Nuovo Cimento Suppl. **3**, 760 (1956).
[20]C. Y. Prescott, W. B. Atwood, R. L. A. Cottrell *et al.*, Phys. Lett. **77B**, 347 (1978); **84B**, 524 (1979).
[21]A. Argento, A. C. Benvenuti, D. Bollini *et al.*, BCDMS Collaboration, Phys. Lett. **120B**, 245 (1983).
[22]A. V. Radyushkin, Fiz. Elem. Chastits At. Yadra **14**, 58 (1983) [Sov. J. Part. Nucl. **14**, 23 (1983)].
[23]T. Sloan, G. Smadja, and R. Voss, Phys. Rep. **162**, 45 (1988).
[24]A. C. Benvenuti, D. Bollini, G. Bruni *et al.*, BCDMS Collaboration, Phys. Lett. **223B**, 490 (1989).
[25]A. A. Akhundov, D. Yu. Bardin, and N. M. Shumeĭko, Yad. Fiz. **26**, 1251 (1977); **44**, 1517 (1986) [Sov. J. Nucl. Phys. **26**, 660 (1977); **44**, 988 (1986)]; D. Yu. Bardin and N. M. Shumeĭko, Yad. Fiz. **29**, 969 (1979) [Sov. J. Nucl. Phys. **29**, 499 (1979)]; A. A. Akhundov, D. Y. Bardin, W. Lohmann, Communication E2-86-104, JINR, Dubna (1986).
[26]L. N. Hand, Phys. Rev. **129**, 1834 (1963).
[27]W. R. Ditzler, M. Breidenbach, J. I. Friedman *et al.*, Phys. Lett. **57B**, 201 (1975).
[28]V. I. Zakharov and N. N. Nikolaev, Yad. Fiz. **21**, 434 (1975) [Sov. J. Nucl. Phys. **21**, 227 (1975)]; N. N. Nikolaev and V. I. Zakharov, Phys. Lett. **55B**, 397 (1975).
[29]J. J. Aubert, G. Bassompierre, K. H. Becks *et al.*, EMC Collaboration, Nucl. Phys. **B293**, 740 (1987).
[30]K. Bodek and J. L. Ritchie, Phys. Rev. D **23**, 1070 (1981); **24**, 1400 (1981); L. L. Frankfurt and M. I. Strikman, Nucl. Phys. **B181**, 22 (1981); J. Berlad, A. Dar, and G. Eliam, Phys. Rev. D **22**, 1547 (1980); W. B. Atwood and G. B. West, Phys. Rev. D **7**, 773 (1973).
[31]J. S. Poucher, M. Breidenbach, and R. Ditzler, Phys. Rev. Lett. **32**, 118 (1974).
[32]A. Bodek, D. L. Dubin, J. E. Elias *et al.*, Phys. Lett. **51B**, 417 (1974).
[33]A. Bodek, M. Breidenbach, D. L. Dubin *et al.*, Phys. Rev. D **20**, 1471 (1979).
[34]G. Smadja, *Proc. of the 1981 Intern. Symposium on Lepton and Proton Interactions at High Energies, Bonn, Aug. 24–29*, edited by W. Pfeil (1981), p. 440.
[35]F. Eisele, *Proc. of the 21st Intern. Conf. on High Energy Physics, Paris, July 26–31, 1982*, edited by P. Petiau and M. Porneuf (1982), p. 337.
[36]A. Bodek, N. Giokaris, W. B. Atwood *et al.*, Phys. Rev. Lett. **50**, 1431 (1983).
[37]A. Bodek, M. Breidenbach, D. Dubin *et al.*, Phys. Rev. Lett. **30**, 1087 (1973).
[38]A. Bodek, N. Giokaris, W. B. Atwood *et al.*, Phys. Rev. Lett. **51**, 534 (1983).
[39]R. G. Arnold, P. E. Bosted, C. C. Chang *et al.*, Phys. Rev. Lett. **52**, 724 (1984).
[40]A. C. Benvenuti, D. Bollini, G. Bruni *et al.*, BCDMS Collaboration, Phys. Lett. **195B**, 91, 97 (1987).
[41]J. J. Aubert, G. Bassompierre, K. H. Becks *et al.*, EMC Collaboration, Nucl. Phys. **B259**, 189 (1985).
[42]J. J. Aubert, G. Bassompierre, K. H. Becks *et al.*, EMC Collaboration, Nucl. Phys. **B272**, 158 (1986).
[43]P. D. Meyers, Measurement of the Nucleon Structure Function in Iron Using 215 and 93 GeV Muons, Ph. D. Thesis, LBL-17108, Berkeley (1983).
[44]Y. Sacquin, *Proc. of the 29th Rencontre de Moriond*, Vol. 2, edited by J. Tran Thanh Van (Editions Frontières, 1984), p. 659.
[45]I. A. Savin and G. I. Smirnov, Brief Communications, No. 2, JINR, Dubna (1984), p. 3; I. A. Savin and G. I. Smirnov, Phys. Lett. **145B**, 438 (1984).
[46]S. Dasu, P. de Barbaro, and A. Bodek, University of Rochester Report UR-1045, April (1986).
[47]G. Bari, A. C. Benvenuti, D. Bollini *et al.*, BCDMS Collaboration, Phys. Lett. **163B**, 282 (1985).
[48]J. Ashman, B. Badelek, G. Baum *et al.*, Phys. Lett. **202B**, 603 (1988).
[49]A. C. Benvenuti, D. Bollini, G. Bruni *et al.*, BCDMS Collaboration, Phys. Lett. **189B**, 483 (1987).
[50]S. Stein, W. B. Atwood, E. D. Bloom *et al.*, Phys. Rev. D **12**, 1884 (1975).
[51]S. Dasu, P. de Barbaro, A. Bodek *et al.*, Phys. Rev. Lett. **60**, 2591 (1988).
[52]D. O. Caldwell, J. P. Cumalat, A. M. Eisner *et al.*, Phys. Rev. Lett. **42**, 553 (1979).
[53]D. Schildknecht, Springer Tracts Mod. Phys. **63**, 57 (1972).
[54]M. Arneodo, A. Arvidson, J. J. Aubert *et al.*, EMC Collaboration, Phys. Lett. **211B**, 493 (1988).
[55]M. R. Adams, S. Aid, P. L. Anthony *et al.*, *Proc. of the 25th Intern. Conf. on High Energy Physics* (Singapore, 1990).
[56]J. Guy, B. Saitta, G. Van Apeldoorn *et al.*, Z. Phys. C **36**, 337 (1987).
[57]H. Abramowicz, G. Hansl-Kozanecki, J. May *et al.*, Z. Phys. C **25**, 29 (1984).
[58]T. Kitagaki, S. Tanaka, H. Yuta *et al.*, *Proc. of the 12th Intern. Conf. on Neutrino Physics and Astrophysics*, edited by T. Kitagaki and H. Yuta (Sendai, Japan, 1986), p. 381.
[59]A. E. Asratyan, P. A. Gorichev, V. I. Efremenko *et al.*, Yad. Fiz. **43**, 598 (1986) [Sov. J. Nucl. Phys. **43**, 380 (1986)].
[60]D. Allasia, C. Angelini, M. Baldo-Ceolin *et al.*, Phys. Lett. **107B**, 148 (1981).

[61]T. Kitagaki, S. Tanaka, A. Yamaguchi *et al.*, Phys. Lett. **214B**, 281 (1988).
[62]T. Kitagaki, S. Tanaka, H. Yuta *et al.*, Phys. Rev. Lett. **49**, 98 (1982).
[63]R. Voss, *Proc. of the 11th Intern. Conf. on Neutrino Physics and Astrophysics*, edited by K. Kleinknecht and E. A. Paschos (Dortmund, Germany, 1984), p. 381.

[64]E. V. Shuryak and A. I. Vainstein, Nucl. Phys. **B199**, 451 (1982).
[65]L. F. Abbott, W. B. Atwood, and R. M. Barnett, Phys. Rev. D **22**, 582 (1980).
[66]V. A. Bednyakov, I. V. Zlatev, Yu. P. Ivanov *et al.*, Yad. Fiz. **40**, 770 (1984) [Sov. J. Nucl. Phys. **40**, 494 (1984)].
[67]Yu. P. Ivanov and P. S. Isaev, Yad. Fiz. **38**, 744 (1983) [Sov. J. Nucl. Phys. **38**, 443 (1983)].
[68]E. V. Shuryak, Nucl. Phys. **A446**, 259 (1985).
[69]A. Benvenuti, D. Bollini, G. Bruni *et al.*, BCDMS Collaboration, Phys. Lett. **223B**, 485, 490 (1989).
[70]R. Windmolders, *Proc. of the 24th Intern. Conf. on High Energy Physics*, edited by R. Kotthaus and J. H. Kuhn (Springer-Verlag, Munich, 1989).
[71]R. P. Bickerstaff and G. A. Miller, Phys. Rev. D **34**, 2890 (1986).
[72]K. Rith, Nucl. Phys. **A446**, 459c (1985).
[73]L. Frankfurt and M. Strikman, Nucl. Phys. **B250**, 143 (1985).
[74]R. Machleid, K. Holinde, Ch. Elster *et al.*, Phys. Rep. **149**, 1 (1987).
[75]L. P. Kaptar', B. L. Reznik, A. I. Titov, and A. Yu. Umnikov, Pis'ma Zh. Eksp. Teor. Fiz. **47**, 428 (1988) [JETP Lett. **47**, 508 (1988)].
[76]O. Nachtmann and H. J. Pirner, Z. Phys. C **21**, 277 (1984).
[77]A. Bodek and A. Simon, Z. Phys. C **29**, 231 (1985).
[78]S. Dasu *et al.*, Universiy of Rochester Preprint UR 1045, Apr. (1988); S. Rock *et al.*, *Proc. of the 24th Intern. Conf. on High Energy Physics*, edited by R. Kotthaus and J. H. Kuhn (Springer-Verlag, Munich, 1989), p. 999.
[79]I. A. Savin, in *Proc. of the Sixth International Seminar on Problems of High Energy Physics*, D1. 2-81-728 [in Russian] (Dubna, 1981), p. 223.
[80]P. Berge, H. Burkhardt, F. Dydak *et al.*, CDHSW Collaboration, Z. Phys. C **49**, 178 (1991).
[81]G. I. Smirnov, *Proc. of the Tenth Intern. Seminar on High Energy Physics Problems*, Sept. 24–29 (Dubna, 1990).
[82]L. Frankfurt and M. Strikman, Phys. Rep. **160**, 235 (1988).
[83]S. Date, K. Saito, H. Sumiyoshi, and H. Tezuka, Phys. Rev. Lett. **52**, 2344 (1984); K. Saito and T. Uchiyama, Z. Phys. A **322**, 299 (1985); Tohoku University Preprint (1985).
[84]M. S. Goodman, M. Hall, W. A. Loomis *et al.*, Phys. Rev. Lett. **47**, 293 (1981).
[85]D. I. Blokhintsev, Zh. Eksp. Teor. Fiz. **33**, 1295 (1957) [Sov. Phys. JETP **60**, 700 (1958)].
[86]L. S. Azhgireĭ, I. K. Vzorov, V. P. Zrelov *et al.*, Zh. Eksp. Teor. Fiz. **33**, 1185 (1957) [Sov. Phys. JETP **60**, 641 (1958)].
[87]A. M. Baldin, in *Proc. of the Fourth International Conference on High Energy Physics and Nuclear Structure* [in Russian], edited by V. P. Dzhelepov (JINR, Dubna, 1971), p. 632.
[88]A. M. Baldin, *Particles and Fields–1971. Proc. of the Rochester Meeting APS/DPF* (New York, 1971), p. 131.
[89]A. M. Baldin, S. B. Gerasimov, N. Gnordanesku *et al.*, Yad. Fiz. **18**, 79 (1973) [Sov. J. Nucl. Phys. **18**, 41 (1974)].
[90]A. M. Baldin, *Proc. of the Intern. Conf. on Extreme States in Nuclear Systems*, Vol. 2 (Dresden, 1980), p. 1.
[91]V. S. Stavinskiĭ, Communication R2-9528 [in Russian], JINR, Dubna (1976).
[92]A. M. Baldin, Yu. A. Panebrattsev, and V. S. Stavinskiĭ, Dokl. Akad. Nauk SSSR **279**, 1352 (1984) [Sov. Phys. Dokl. **29**, 1031 (1984)].
[93]A. M. Baldin, V. K. Bondarev, N. Giordanesku *et al.*, Communication E1-82-472, JINR, Dubna (1982).
[94]I. M. Belyaev, O. P. Gavrishchuk, L. S. Zolin *et al.*, Brief Communication No. 8 [in Russian], JINR, Dubna (1985), p. 29; I. M. Belyaev, O. P. Gavrishchuk, P. I. Zarubin *et al.*, Yad. Fiz. **49**, 473 (1989) [Sov. J. Nucl. Phys. **49**, 295 (1989)].
[95]V. K. Bondarev, P. I. Zarubin, A. G. Litvinenko *et al.*, Brief Communication No. 4 [in Russian], JINR, Dubna (1984), p. 5.
[96]J. J. Aubert, G. Bassompierre, K. H. Becks *et al.*, EMC Collaboration, Phys. Lett. **152B**, 433 (1985).
[97]M. D. Sokoloff, J. C. Anjos, J. A. Appel *et al.*, Phys. Rev. Lett. **57**, 3003 (1986).
[98]L. Anderson, W. W. Ash, D. B. Gustavson *et al.*, Phys. Rev. Lett. **38**, 263 (1977).
[99]R. Baier and R. Rückl, Nucl. Phys. **B218**, 289 (1983).
[100]T. Weiler, Phys. Rev. Lett. **44**, 304 (1980).
[101]S. V. Katsanevas, C. Kurkoumelis, A. Markou *et al.*, Phys. Rev. Lett. **60**, 2121 (1988).
[102]Yu. M. Antipov, V. A. Bessubov, N. P. Budanov *et al.*, Phys. Lett. **72B**, 278 (1977); **76B**, 235 (1978); M. J. Corden, J. D. Dowell, J. Garvey *et al.*, Phys. Lett. **110B**, 415 (1982).
[103]C. H. Chang, Nucl. Phys. **B172**, 425 (1980); R. Baier and R. Rückl, Z. Phys. C **19**, 251 (1982).
[104]L. Clavelli, P. H. Cox, B. Harms, S. Jones *et al.*, Phys. Rev. D **32**, 612 (1985).
[105]J. Qui, Nucl. Phys. **B291**, 746 (1987).
[106]B. Z. Kopeliovich and E. Niedermayer, E2-84-834, JINR, Dubna (1984); B. Z. Kopeliovich, Fiz. Elem. Chastits At. Yadra **21**, 117 (1990) [Sov. J. Part. Nucl. **21**, 49 (1990)].
[107]P. Bordalo, P. H. Busson, L. Kluberg *et al.*, Phys. Lett. **193B**, 368 (1987).
[108]S. V. Akulinichev, S. Kulagin, and G. M. Vagradov, Phys. Lett. **158B**, 485 (1985).
[109]G. L. Li, R. F. Liu, and G. E. Brown, Phys. Lett. **213B**, 531 (1988).
[110]L. L. Frankfurt and M. I. Strikman, Phys. Lett. **183B**, 254 (1987).
[111]P. D. Morley and I. Schmidt, Phys. Rev. D **34**, 1305 (1986).
[112]I. A. Schmidt and R. Blankenbecler, Phys. Rev. D **15**, 3321 (1977).
[113]A. V. Efremov, Phys. Lett. **174B**, 219 (1986).
[114]F. E. Close, R. G. Roberts, and G. G. Ross, Phys. Lett. **129B**, 346 (1983).
[115]R. L. Jaffe, F. E. Close, R. G. Roberts, and G. G. Ross, Phys. Lett. **134B**, 449 (1984).
[116]F. E. Close, R. L. Jaffe, R. G. Roberts, and G. G. Ross, Phys. Rev. D **31**, 1004 (1985).
[117]F. E. Close, R. G. Roberts, and G. G. Ross, Phys. Lett. **168B**, 400 (1986).
[118]R. L. Jaffe, in *Relativistic Dynamics and Quark–Nucleon Physics*, edited by M. B. Johnson and A. Picklesimer (Wiley, 1986), p. 537.
[119]E. M. Levin and M. G. Ryskin, Yad. Fiz. **40**, 809 (1984) [Sov. J. Nucl. Phys. **40**, 519 (1984)].
[120]L. Frankfurt and M. Strikman, Leningrad Institute of Nuclear Physics Reports, No. 886 (1983); No. 929 (1984).
[121]I. A. Savin, in *Proc. of the 22nd Intern. Conf. on High Energy Physics*, Vol. 2, edited by A. Meyer and E. Wieczorek (Leipzig, 1984), p. 251.
[122]G. Chanfray, O. Nachtmann, and H. J. Pirner, Phys. Lett. **147B**, 249 (1984); H. J. Pirner, Comments Nucl. Part. Phys. **12**, 199 (1984).
[123]I. Sick, in *Weak and Electromagnetic Interactions in Nuclei*, edited by H. V. Klapdor (Springer-Verlag, 1987), p. 415; D. Day, J. S. McCarthy, I. Sick *et al.*, Phys. Rev. Lett. **43**, 1143 (1979).
[124]L. Frankfurt and M. Strikman, Leningrad Institute of Nuclear Physics Reports, No. 1329 (1987).
[125]E. G. Drukarev and E. M. Levin, Pis'ma Zh. Eksp. Teor. Fiz. **48**, 307 (1988) [JETP Lett. **48**, 338 (1988)].
[126]J. V. Noble, Phys. Lett. **178B**, 285 (1986).
[127]C. H. Llewellyn-Smith, Phys. Lett. **128B**, 107 (1983).
[128]M. Eriscon and A. W. Thomas, Phys. Lett. **128B**, 112 (1983).
[129]E. L. Berger and F. Coester, Phys. Rev. D **32**, 1071 (1985).
[130]G. G. Arakelyan and K. G. Boreskov, Yad. Fiz. **31**, 1578 (1980); **41**, 416 (1985) [Sov. J. Nucl. Phys. **31**, 819 (1980); **41**, 267 (1985)].
[131]V. K. Luk'yanov and A. I. Titov, Fiz. Elem. Chastits At. Yadra **10**, 815 (1979) [Sov. J. Part. Nucl. **10**, 321 (1979)].
[132]C. W. Wong, Phys. Rep. **136**, 1 (1986).
[133]H. J. Pirner and J. P. Vary, Phys. Rev. Lett. **46**, 1376 (1981).
[134]D. Day, J. S. McCarthy, I. Sick *et al.*, Phys. Rev. Lett. **43**, 1143 (1979).
[135]D. Sivers, S. J. Brodsky, and R. Blankenbecler, Phys. Rep. **23**, 1 (1976).
[136]V. Matveev, R. Muradyan, and A. Tavkhelidze, Lett. Nuovo Cimento **7**, 719 (1973).
[137]R. L. Jaffe, Phys. Rev. Lett. **50**, 228 (1983).
[138]R. L. Jaffe, F. E. Close, R. G. Roberts, and G. G. Ross, Phys. Lett. **134B**, 449 (1984).
[139]A. A. Bondarchenko and A. V. Efremov, E2-84-124, JINR, Dubna (1984).
[140]W. Furmanski and A. Krzywicki, Z. Phys. C **22**, 391 (1984).
[141]J. P. Vary, Nucl. Phys. **A418**, 195 (1984).

[142]C. E. Carlson and T. J. Havens, Phys. Rev. Lett. **51**, 261 (1983).
[143]A. I. Titov, Yad. Fiz. **38**, 1582 (1983); **40**, 76 (1984) [Sov. J. Nucl. Phys. **38**, 964 (1983); **40**, 50 (1984)].
[144]M. Chemtob and R. Peschanski, J. Phys. G **10**, 599 (1984).
[145]V. R. Garsevanishvili and Z. R. Menteshashvili, in *Proc. of the Seventh International Seminar on Problems of High Energy Physics*, D1. 2-84-599 (Dubna, 1984), p. 157.
[146]B. C. Clark, S. Hama, B. Mulligan, and K. Tanaka, Phys. Rev. D **31**, 617 (1985).
[147]K. E. Lassila and U. P. Sukhatme, Phys. Lett. **209B**, 343 (1988).
[148]H. Faissner and B. R. Kim, Phys. Lett. **130B**, 321 (1983).
[149]H. Faissner, B. R. Kim, and H. Reithler, Phys. Rev. D **30**, 900 (1984).
[150]L. A. Kondratyuk and M. Zh. Shmatikov, Pis'ma Zh. Eksp. Teor. Fiz. **39**, 324 (1984) [JETP Lett. **39**, 389 (1984)]; Yad. Fiz. **41**, 498 (1985) [Sov. J. Nucl. Phys. **41**, 317 (1985)].
[151]N. P. Zotov, V. A. Saleev, and V. A. Tsarev, Pis'ma Zh. Eksp. Teor. Fiz. **40**, 200 (1984) [JETP Lett. **40**, 965 (1984)]; Yad. Fiz. **45**, 561 (1987) [Sov. J. Nucl. Phys. **45**, 352 (1987)].
[152]J. Dias de Deus, M. Pimenta, and J. Varela, Phys. Rev. D **30**, 697 (1984); Z. Phys. C **26**, 109 (1984).
[153]S. Date and A. Nakamura, Prog. Theor. Phys. **69**, 565 (1983).
[154]N. P. Zotov and V. A. Saleev, Preprint 89 12/89 [in Russian], Institute of Nuclear Physics, Moscow State University, Moscow (1989).
[155]C. Ishii, K. Saito, and F. Tagaki, Phys. Lett. **216B**, 409 (1989).

Translated by Julian B. Barbour